University of Sussex

Dark Matter Direct Detection from a model with spin-2 mediators

Alba Leticia Carrillo Monteverde

Submitted for the degree of Doctor of Philosophy

University of Sussex

February 2019

Declaration

I hereby declare that this thesis has not been and will not be submitted in whole or in part to another University for the award of any other degree.

Signature:

Alba Leticia Carrillo Monteverde

UNIVERSITY OF SUSSEX

Alba Leticia Carrillo Monteverde

Submitted for the degree of Doctor of Philosophy

Dark Matter Direct Detection from a model with spin-2 mediators

Summary

Dark Matter (DM) and its nature is one of the most interesting problems in modern physics. DM constitutes the 27% of the total content of the Universe and evidence of its existence have been accumulated at diferent scales thanks to its gravitational infuence on ordinary matter. One of the most interesting proposals to study this problem is to assume that DM is made of particles.

We study models where a massive spin-two resonance acts as the mediator between Dark Matter (DM) and the SM particles. The interaction of DM and SM is through the energy-momentum tensor and we explore the scenarios where DM is a fermion, a scalar and a vector field.

We identify the effective interactions when the mediator is interated out, and match them to the gravitational form factors in order to study the DM-nucleon scattering that will be helpful in the phenomenological analysis.

Up to this day, only gravitational efects of DM have been observed but we hope to obtain information that will help us to identify its nature through these three different approaches: direct detection searches, indirect detection techniques and production at colliders. In the context of this work, we obtain the limits on the parameter space of the Gravity Mediated Dark Matter model using the relic density conditions, direct detection bounds and collider searches for the spin-two mediator.

Acknowledgements

I want to start saying thank you to the most important people in my life, my family. My mother Lety, my father Julio, Julio, Oiluj, Bambam and my chosen one, Lao. I love you with all my heart and without you by my side I wouldn't be able to finish my work. Your inconditional love and support kept me going even in the hardest times. And Lao, I know that we had some of those times but I am so happy that we went against the odds and until this day, we keep growing together.

Also, I want to give a very special recognition to my supervisor, Veronica Sanz. She is the best supervisor in the world and I know that I was not the student she deserved but I will always say thank you because you always did your best to understand me during all this time, to show me your support, to share your knowledge and I appriciate all the advices I received from you. You are a role model for me.

To my collaborators in South Korea, Hyun Min Lee, Myeonghun Park and Yoo-Jin Kang, thank you for your hard work and great ideas, all the interesting discussions and for always finding a good time to settle a Skype meeting.

I want to thank CONACYT and the people of Mexico for the opportunity to do my PhD abroad granting me a scholarship and I hope that many people like me can still have this chances in the future. I want to pay you back being a good citizen and a good physicist in order to contribute to make our country a better place. I'll do my best.

I want to thank all the people from the Physics Department at Sussex that I had the pleasure to share something during my time here. Specially to my officemates and friends that made my expirience in campus a really good one.

And to all my Mexican and non Mexican friends in the UK that shared during these 4 years some great moments cooking, dancing, singing, traveling and even just walking around, I can say to you that I appreciate all the things you brought to my life in this place far away from home. You made it warmer and fun. I hope to see all of you again.

I want to mention some very special people for me. My extended family and friends back in Mexico that always receive me with open arms in Hermosillo, Pachuca, Puebla and Mexico City. And finally, those that are not with us anymore that I will always remember

and keep in my heart.

And to you that for some reason are reading this work (even if I mention you before), I hope that we share our love for nature and the mysteries of the Universe.

Contents

List of Tables

List of Figures

Chapter 1

Introduction

The nature of Dark Matter (DM) is one of the biggest mysteries in physics nowadays as it represents a big part of the matter content of our galaxy and the Universe in general. According to the measurement made by Planck, it constitutes the 27% of the Universe [1] and the only effect that provide us of evidence of its existence came from the gravitational effect on the visible matter.

It was proposed as a solution of different astronomical and cosmological observations that were deviated from the predictions made by the theory and until this day it is the best explanation to most of these observed discrepancies [2]. As for visible matter, the approach behind the DM idea from a particle physics point of view is that DM is made out of particles. The Standard Model (SM) is the model that describes all the fundamental particles and their interactions but we know it has some problems that need to be fixed and for this reason we have proposed extensions or some new models that contain the SM at a different scale. Models Beyond the SM usually contain one or more particles that can potentially play the role of a DM component but not all models can pass the necessary requirements [3].

The interaction of DM and the SM is useful as we want to be able to identify its nature. In some models, this interaction happens using a particle as a portal or through electroweak interactions, this means that DM can annihilate or decay into SM particles, but signals of these type of interactions have not been observed.

Different techniques are used in order to detect the corresponding signals [4]. The three main approaches are direct detection, where the DM particle interacts directly with the matter in our detector provoking an effect that can be measured; indirect detection consists in observing the products produced by the decay or annihilation of DM in some place in the Universe and these products can be gamma rays, protons, positrons, neutrinos and

other particles, each type with a corresponding footprint that allow us to say something about the original particle or particles; and finally, the production of DM in colliders that would result in some particular signals in the event reconstructions as missing energy and mono jets. More details of this discussion are describe in chapter 2. Also, it is presented a brief description of the different strategies in current and future experiments for direct detection and also how to compute the detection rates.

In this work, we use the fact that only gravitational interaction has been observed between visible and dark matter to study the possible signals on direct detection experiments. The Gravity Mediated Dark Matter (GMDM) model can be a good set up to explain DM-SM interactions. In this model, DM only interacts with the SM content through the exchange of gravity mediators [5], in particular the graviton that came from the compactification of a warped 5-dimension. The model is described a bit more in chapter 3 with a brief discussion about the dual description of this type of models.

To be able to do this study, in chapter 4 you can find the corresponding effective field theory of the interaction of different types of DM with the nucleons in order to do a complete computation of the limits on the nucleon-DM cross section over the parameter space of the GMDM model, the computation of the differential event rates for different nuclei and different experiments [6] and also the effect of the relic abundance of the DM candidate in this scenario that will allow to set constrains on the parameter space of the model as well.

Finally, the conclusions obtained for this study are described in chapter 5.

Chapter 2

Dark Matter searches

In this chapter, a general introduction to the problem of Dark Matter is given, starting with a bit of the historic background and the evidence of its existence. Also, a quick review of the main points to consider a particle a good candidate for DM and some examples. And finally, an introduction of the different detection techniques is described.

2.1 The dark nature of Dark Matter and the evidence of its existence

Dark Matter (DM) is one of the main components of the Universe and corresponds to the 27% of the total amount of energy in it [1]. As its name states, we call this matter dark because it cannot emit or absorb light and for this reason, the only effect that we have observed is the gravitational effect over other bodies at different scales [2].

This concept of DM was introduced to explain the discrepancies observed in the movement of luminous objects in the sky at different scales, as the stars in a galaxy or galaxies in a cluster, and the predictions from the established theory, Newton's gravitational theory, that work very well to explain the physical phenomena at large scale. The collection of evidence coming from the astronomical observations that we are talking about are going to be explained below in more detail.

The first evidence corresponds to the studies in the 30's of Fritz Zwicky [7]. Measuring the mass of a system, as a galaxy cluster, is very difficult to do in a direct way but using the virial theorem, that postulates the relation between the average kinetic energy of a bound system with the average gravitational potential, it is possible to find a relation between mass and the radial velocity of the bodies in the system, that can be measured easily thanks to the Doppler shift. Zwicky studied the radial velocities of different galaxies

in the Coma Cluster and he observed that these galaxies seem to move faster than the amount of observed matter will allow using the virial theorem. He computed the mass of these objects and he found that the mass needed to explain this movement was bigger than the amount computed from the visible galaxies. To solve this discrepancy, he proposed that invisible matter was the reason behind the observations but the community thought that this discrepancy will be fixed once the tools and techniques improve with time.

It was until 1960 when Jean Oort concluded that the discrepancy measured by Zwicky was real and then we start thinking that an additional component of the interstellar medium could exist that has not been detected yet.

The second evidence, and the one that it is called the first significant clue of a discrepancy at the galactic scale, corresponds to rotation curves of galaxies [8]. Rotation curves are graphs that show the angular velocity of the stars and gas in a galaxy as a function of the distance to the center of the galaxy. The curves are obtained tracking of the movement of hydrogen, the main component of stars. In Figure 2.1, we can see the predicted behaviour compared with the measurements of the spiral galaxy M33. The predicted behaviour can be explained if we compared the the gravitational potential with the kinetic energy of a star in the galaxy. In this case, $V = \frac{-GM}{r}$ and $K = \frac{1}{2}mv^2$ and combining this two expressions we can find the relation between the velocity and the distance to the center of the galaxy as $v = \sqrt{\frac{2G}{r}}$. That is the dotted line in the Figure 2.1.

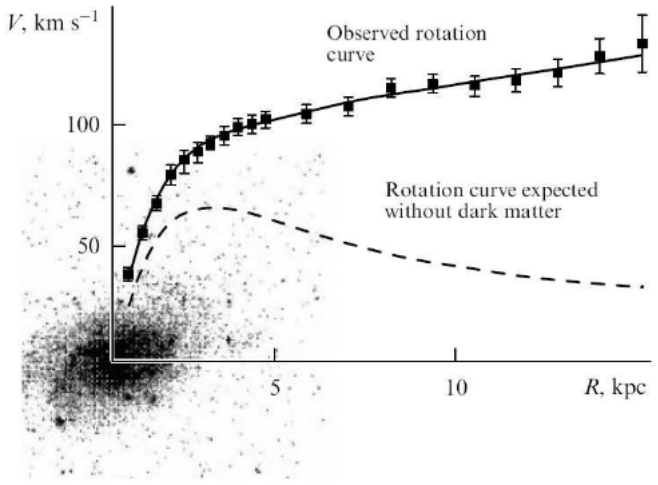

Figure 2.1: This is the rotation curve of the of the M33 galaxy [9].

The third one corresponds to gravitational lensing. In this case, the Bullet cluster is an important example of this phenomena. The Bullet Cluster is a pair of galaxy clusters that are colliding and during the process, it was observed that the effect of gravitational

lensing occurs not in the area where the dust and gas are interacting but the effect is observed in the outer part. This is difficult to explain if we consider that there is only stars, gas and dust involved in the collision as a very large amount of mass is required to be located in the area where the lensing effects is observed, therefore this indicates that invisible, non interacting and very massive matter pass through during the collision and now its located in the area where we can see its effect.

And the fourth evidence corresponds to the development of simulations of the Universe. Scientist that try to replicate the right structure of the universe in the present days through the numerical solution of the evolution equations consider for their simulation DM as the main matter component. This is, it is necessary to include in the simulations the right amount of DM and let it evolve in time to obtain the observed structure of the Universe. In Figure 2.2, the Millenium simulation is shown as an example of these remarkable results [10].

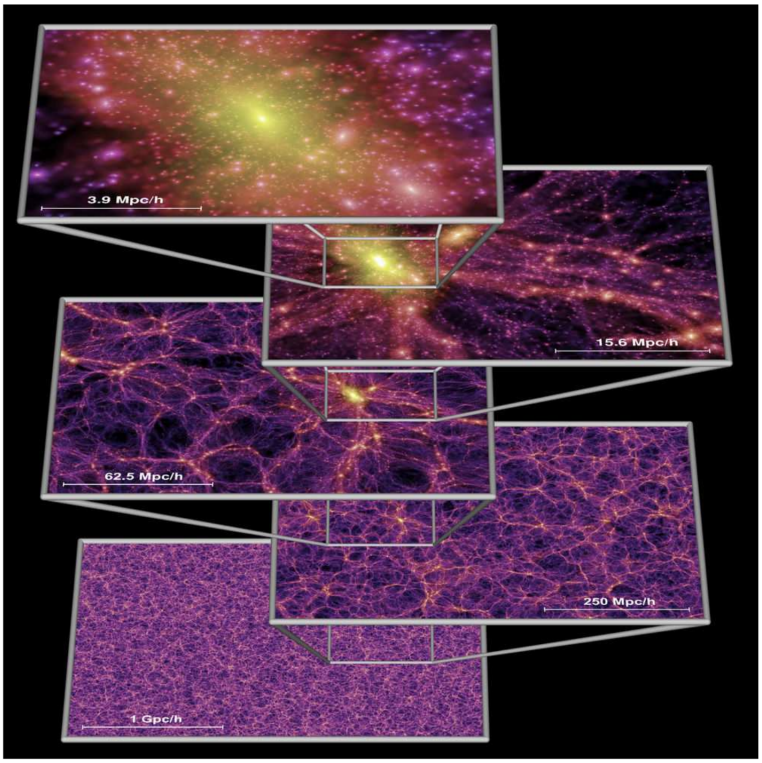

Figure 2.2: The dark matter density field on various scales. The zoom sequence displays consecutive enlargements byfactors of four, centred on one of the many galaxy cluster halos present in the simulation [10].

2.2 DM candidates

The model that describes all the visible matter that we know is the very successful Standard Model of Particle Physics. Despise that up until now this model describes very well all the experimental measurements done at the colliders, we know it has unsolved and very important questions that need to be explained. Among the problems, we have the mass of the neutrinos and the hierarchy problem just to mention some of them. New extensions to the SM are proposed to solve one or more of these issues.

Depending of the way how DM particles moves, it can be classified in 3 types: cold, warm and hot. Their velocities are directly related with the size and mass of the particles and also with the.

The problem that we are interested in this work is Dark Matter nature. Unfortunately, the SM does not contain a particle that is a good candidate to be the main component of cold DM. Neutrinos were once thought as the SM candidate but they have been ruled out as their velocities are near the speed of light and then it cannot form structures as it is observed in the Universe but still these particles can be consider part of warm or hot dark matter that it is not being consider in this work [3].

Cold DM is the component of DM that moves at non relativistic velocities and it is the reason behind the formation of structure in the Universe. Many of the models beyond the SM contain one or more particles that can be considered to be DM but not all of them can pass the tests [3].

As it was mentioned by Taoso, Bertone and Masiero, these particles need to satisfy a list of probes:

- Do they give the right relic abundance?
- Are they cold?
- Are they neutral?
- Is it self-interactive?
- Do they change the formation of structure?
- Do they change the results from BBN?
- Is it possible to observe it?

A special remark on the observational aspects of this test is considered as it is expected to be able to identify the nature of the particle or particles that form DM using all the

different strategies that scientists have developed for this matter.

Some of the most popular candidates are the weakly interactive massive particles or WIMPS and this type of particles can be part of very well known BSM models as SUSY, models with extra dimensions and more. Also, there are some popular candidates with very small masses too, as the axions [11].

The easiest way to try to explain the DM content is using only one type of particle to explain the evidence but this is just the first path as there is no evidence that support this idea as the DM can be formed by a variety of particles as it is the case for visible matter but only experiments and astronomical observations can give us the right answer.

2.3 Relic Abundance

After the Big Bang, most of the Universe's constituents were in thermal equilibrium and departures from this equilibrium led to important relics. For example, from neutrino decoupling we observed now a neutrino background, or from the decoupling of background radiation we now observe the Cosmic Microwave Background (CMB) [2].

If a particle species was in thermal equilibrium, as the Universe expands, there is a point when it can decouple from the plasma, in other words, it is no longer in thermal equilibrium and reaches the thermal freeze out.

Once the species decouple, its particle number density evolution is decreasing as R^{-3}, where R is the scale factor of the Universe.

The freeze out happens when the rate of annihilation and creations of this species drops below the expansion rate of the Universe and therefore the density remains constant. This means than in some stage, the annihilations and creations of the particle were more frequent and this frequency decreased as the Universe is expanding until some point that it is very difficult for a particle to interact and then its density freezes and remains constant. This comoving density is called the relic abundance of a certain species of particles.

In the case of DM, this density corresponds to a value of $\Omega h^2 = 0.1199$.

The current value of Ω_{DM} is obtained indirectly from the fit of the global cosmic parameters from different observations as the CMB anisotropies, the galaxies spacial distributions, and other astrophysical observations [12].

To obtain the density of particles of a certain specie is necessary to solve the Boltzmann equation. This equation is the rule for the evolution of the distribution function as it can be written as an equation for the number of particles as it is shown in different references

as [2,3]. The Boltzmann equation is

$$\mathbf{L}[f] = \mathbf{C}[f], \tag{2.1}$$

where $\mathbf{L}$ is the Liouville operator, $\mathbf{C}$ is the collision operator and f is phase space distribution function of the species that decoupled.

If the Friedman-Robertson-Walker model is considered, the phase space is homogeneous and isotropic, this means that f is a function of the Energy and time,

$$f = f(|\vec{p}|, t) = f(E, t), \tag{2.2}$$

and considering also the Robertson-Walker metric in the Liouville operator, it can be written in the following form

$$\hat{L}[f(E,t)] = E\frac{\partial f}{\partial t} - \frac{\dot{R}}{R}|\vec{p}|^2\frac{\partial f}{\partial E}. \tag{2.3}$$

The number density is defined in terms of the phase space density as follow

$$n(t) = \frac{g}{(2\pi)^3}\int d^3p f(E,t), \tag{2.4}$$

where g is the number of internal degrees of freedom. Using this definition and integration by parts on equation 2.3, we can write the Boltzmann equation 2.1 in the following form

$$\frac{dn}{dt} + 3\frac{\dot{R}}{R}n = \frac{g}{(2\pi)^3}\int \frac{d^3p}{E}\mathbf{C}[f(E,t)]. \tag{2.5}$$

To write down the form of the right-hand side of this equation, consider that the process of interest for the species of particles ψ, whose evolution we are focusing on, is $\psi + a + b + \cdots \leftrightarrow i + j + \cdots$.

The collision term for this process is

$$\begin{aligned}\frac{g}{(2\pi)^3}\int \frac{d^3p}{E}\mathbf{C}[f] \quad = \quad & -\int d\Pi_\psi d\Pi_a d\Pi_b \cdots d\Pi_i d\Pi_j \cdots (2\pi)^4\delta^4(P_\psi + P_a + P_b + \cdots - P_i - P_j - \cdots) \\ & \left[\mathcal{M}^2_{\psi+a+b+\cdots\leftrightarrow i+j+\cdots} f_a f_b \cdots f_\psi (1 \pm f_i)(1 \pm f_j)\cdots\right. \\ & \left. -\mathcal{M}^2_{i+j+\cdots\leftrightarrow\psi+a+b+\cdots} f_i f_j \cdots (1 \pm f_a)(1 \pm f_b)\cdots(1 \pm f_\psi)\right],\end{aligned} \tag{2.6}$$

where $f_{\psi,a,b,\cdots,i,j,\cdots}$ are the phase space densities of species $\psi, a, b, \cdots, i, j, \cdots$, the signs $(+)$ applies for bosons, $(-)$ for fermions, δ^4 enforces energy and momentum conservation, $\mathcal{M}^2$ is the matrix elements squared of the corresponding process and it is averaged over initial and final spins and also includes the appropriate symmetry factors for identical particles and

$$d\Pi \equiv \frac{g}{(2\pi)^3}\frac{d^3p}{2E}. \tag{2.7}$$

In order to simplify the previous equation, some assumptions are considered. First, in our problem, only one or two species will have equilibrium phase space distribution functions so the set of integral-partial differential equations is reduced to a single equation for the specie of interest. Second, CP invariance is considered and then $\mathcal{M}^2_{i+j+\cdots\to a+b+\cdots+\psi} = \mathcal{M}^2_{\psi+a+b+\cdots\to i+j+\cdots} \equiv \mathcal{M}^2$. And third, Maxwell-Boltzmann statistics is used for all species.

Therefore, in the absence of Bose condensate or Fermi degeneracy, the factor $(a \pm f) \approx 1$ and we can write the phase space densities for all species in kinetic equilibrium as

$$f_i(E_i) = \exp(-(E_i - \mu_i)/T). \tag{2.8}$$

Finally, Boltzmann equation can be written as

$$\begin{aligned} \dot{n_\psi} + 3Hn_\psi &= -\int d\Pi_\psi d\Pi_a d\Pi_b \cdots d\Pi_i d\Pi_j \cdots (2\pi)^4 \delta^4(P_i + P_j + \cdots - P_a - P_b - \cdots - P_\psi) \\ &\quad (f_a f_b \cdots f_\psi - f_i f_j \cdots). \end{aligned} \tag{2.9}$$

This can be written also as

$$\frac{dn}{dt} + 3Hn = -\langle \sigma v \rangle \left(n^2 - (n^{eq})^2 \right), \tag{2.10}$$

where σv is the total annihilation cross section times velocity, the brackets means the thermal average, H is the Hubble parameter and n^{eq} is the particle density in thermal equilibrium.

For Cold DM, we are talking about massive particles moving at non relativistic velocities so using the Maxwell-Boltzmann approximation we have

$$n^{eq} = g \left(\frac{mT}{2\pi} \right)^{3/2} \exp^{-m/T}, \tag{2.11}$$

where m is the particle mass and T is the temperature.

Now, changing the variable

$$Y \equiv \frac{n}{s},\ Y^{eq} \equiv \frac{n^{eq}}{s}, \tag{2.12}$$

where s is the entropy density $s = 2\pi^2 g_* T^3/45$ and g_* is the number of relativistic degrees of freedom,and using the conservation of entropy per volume ($sa^3 = constant$), we get

$$\dot{n} + 3Hn = s\dot{Y}, \tag{2.13}$$

and then

$$s\dot{Y} = -\langle \sigma v \rangle s^2 \left(Y^2 - (Y^{eq})^2 \right). \tag{2.14}$$

Now, we can do another change of variables $x \equiv m/T$ so we can write the previous equation as

$$\frac{dY}{dx} = -\frac{\langle \sigma v \rangle \, s}{Hx} \left(Y^2 - (Y^{eq})^2 \right). \tag{2.15}$$

For non relativistic heavy states, we can use the approximation of $\langle \sigma v \rangle$ as an expansion in powers of the non-relativistic velocity v^2

$$\langle \sigma v \rangle = a + b\langle v^2 \rangle + O(\langle v^4 \rangle) \approx a + 6b/x, \tag{2.16}$$

and using $\triangle = Y - Y^{eq}$, we finally obtain

$$\triangle' = -Y^{eq'} - f(x) \triangle (2Y^{eq} + \triangle), \tag{2.17}$$

where the prime sign means the derivative d/dx and

$$f(x) = \sqrt{\frac{\pi g_*}{45}} \, m \, M_{pl} \, (a + 6b/x) \, x^{-2}. \tag{2.18}$$

Introducing the quantity $x_F \equiv m/T_F$, where T_F is the freeze out temperature of the relic particle, it is possible to solve analytically the previous equation in two limits, before the freeze out $x \ll x_F$ and after the decoupling $x \gg x_F$

$$\triangle = -\frac{Y^{eq'}}{2f(x) \triangle^2 Y^{eq}} \text{ para } x \ll x_F, \tag{2.19}$$

$$\triangle' = -f(x) \triangle^2 \text{ para } x \gg x_F. \tag{2.20}$$

Integrating the last equation between the values x_F and ∞ and using $\triangle_{x_F} \gg \triangle_\infty$, we can obtain the value $\triangle_\infty$ and we get

$$Y_\infty^{-1} = \sqrt{\frac{\pi g_*}{45}} M_{Pl} \, m \, x_F^{-1} (a + 3b/x_F). \tag{2.21}$$

For a generic specie of particles X, the solution is

$$\rho_X = m_X n_X = m_X s_0 Y_\infty, \tag{2.22}$$

where $s_0 = 2889.2 \text{ cm}^{-3}$ is the entropy density nowdays when we assume that there are three species of neutrinos. The relic density can be finally written in terms of the critical density as

$$\Omega_X h^2 \approx \frac{1.07 \times 10^9 \text{ GeV}^{-1}}{M_{Pl}} \frac{x_F}{\sqrt{g_*}} \frac{1}{(a + 3b/x_F)}, \tag{2.23}$$

where a and b are expressed in GeV^{-2} and g_* is evaluated at the freeze out temperature. As a convention, we write the density in terms of the Hubble parameter $h = H_0/100 \, km \, s^{-1} \, Mpc^{-1}$.

To complete the calculation of the relic density, we need to compute the annihilation cross section and from this we can extract the parameters a and b which depend on the mass of the DM particle.

Sometimes it is useful to do an estimation of the order of magnitude of the relic density and for this we can use the following approximation [13]:

$$\Omega_X h^2 \approx \frac{3 \times 10^{-27}\ \text{cm}^3\, s^{-1}}{\langle \sigma v \rangle}. \tag{2.24}$$

2.4 Detection techniques

Even if DM does not absorb or emit radiation that can be observed with our telescopes, we hope to be able to identify its nature in other ways, this is through the weak interaction with the SM particles or through new interactions beyond the standard model, as portals. There are a few ways to detect DM and a brief introduction to some of the different approaches is discussed in this section.

The following diagram from 2.4 is very useful when the different mechanisms of detection of DM are explained.

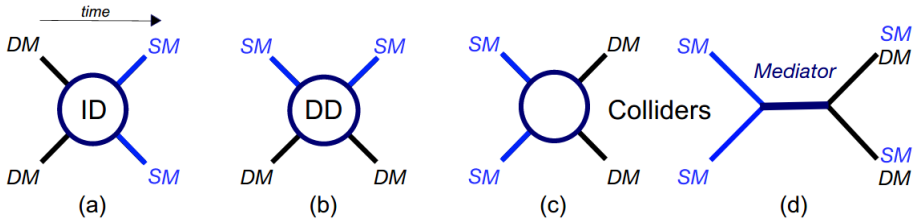

Figure 2.3: Schematic illustration of DM interactions and their corresponding experimental detection techniques. Fig.(a) shows Indirect detection experiments that study DM annihilation to SM particles. Fig. (b) shows the scattering of DM and SM particles used in Direct Detection experiments. Fig. (c) shows the production of DM particles at colliders from the annihilation of SM particles. And Fig. (d) shows the interaction through a mediator particle between DM and SM particles. This process is also a production mechanism of DM in colliders and if the theory predicts the creation of DM through some mediator, then the inverse process will also occur [14].

For the experiments of direct and indirect detection there are two quantities that are very important to compute the rates of detection. The first one is the density of DM and the first estimation of this quantity was done by J. H. Jeans in 1922 [2]. In direct detection it is very important to know the density in our local region in the Milky Way but for some

other type of experiments, it is important to know the distribution of DM in the galactic halo. The local DM density is considerably well known compared for example with the density in the galactic center, and it corresponds to $\rho_0 = 0.3\,\mathrm{GeV/cm^3}$ [2]. This density is determined through the observation of the rotation curves. In particular, it is very hard to measure the Milky Way rotation curve due to our position in the galaxy.

The second quantity needed is the velocity distribution of DM as a function of the distance to the center of the galaxy and it is computed again using the measurements of the rotation curves. For direct detection the local value is relevant and we have that the mean velocity is $\bar{v} = \langle v^2 \rangle^{1/2} \cong 270\,km/s$. In chapter **??**, this subject is explained in more detail.

In the followind sections the three mechanisms will be described but direct detection is explained in more detail as it is one of the main focus of this thesis.

2.4.1 DM production at colliders

This section is about how we use colliders to probe the existence of DM. In this case, it is expected that DM particles can be produce in colliders, like the Large Hadron Collider (LHC) at CERN, from the collision of SM particles and these processes would leave a particular signal when we reconstruct the corresponding events. As in these experiments, the total momentum is expected to be zero and considering that DM should be stable and live as long as the age of the Universe, the main signals of DM production correspond to missing transverse energy as the WIMPs can escape from all the different detector layers leaving no trace as these particles do not interact strongly or electromagnetically with the mass of the detector. Missing transverse energy has been a very relevant tool in the process of discover new particles, for example, the W boson was discovered using this approach in the UA1 experiment in 1983. Also, other way used to search for DM particles is the observation of deviations in the Higgs invisible width and other SM prediction in events called mono-X, where X can be W or Z bosons, photons and leptons.

Many different signatures employed to search for DM at LHC, will become especially relevant if a signal is observed in any DM detection experiments as collider searches are highly complementary to the other detection methods as they cannot determine if what they see is the DM or any other neutral particle as all of them can pass outside the detector and can be seen as missing energy. The main advantage of collider detections is that these measurements do not suffer from astrophysical uncertainties and that there is no lower limit to their sensitivity on DM masses.

The leading generic diagrams responsible for DM production at colliders involve the pair-production of WIMPs and a gluon, photon or a weak gauge boson Z, W in the initial or final state, which is necessary to balance the momentum of the WIMPs so that they are not produced back-to-back resulting in negligible missing energy. Therefore, the search is based on selecting events with high missing energy due to the WIMPs and a single jet (monojet), photon (monophoton) or boson candidate.

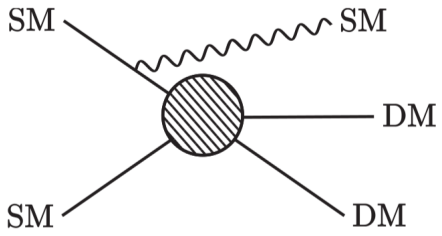

Figure 2.4: This diagram illustrates the process of DM production at the collider. It is necessary to produce DM in association with SM states in order to observe these signals.

2.4.2 Indirect detection

The indirect detection techniques tries to observe the particles produced in the annihilation or decay of DM particles. These products can be antiprotons, positrons, gamma rays or neutrinos. Depending on the nature of the secondary particles, we have different types of experiments.

Gamma ray observation is a very popular way to try to identify what DM is made of as these particles travel in the space without being absorbed for the interstellar medium and it is considered a smoking gun for DM detection since no other known physical processes can give rise to similar signal. Another interesting feature is that the energy spectrum of the photons is related directly with the mass of the original particles. Gamma rays observatories like Fermi-LAT [**?**], that is an imaging high-energy gamma-ray telescope located as the primary instrument in the Fermi spacecraft launched into a near-earth orbit on 11 June 2008; or the High Altitude Water Cherenkov (HAWC) [**?**], a facility located in Sierra Negra volcano near Puebla, Mexico, and other are able to measure a broad spectrum of gamma rays coming from different regions in the sky.

As we have no idea if DM is a completely stable particle or just its life time is longer than the age of the Universe, in some extensions of the Standard Model that contain DM candidates, the stability of the DM particles is guaranteed imposing a symmetry that prohibits its decay. But its important to notice that the signals coming from annihilation

or decays need different detection strategies.

To improve the probabilities to detect particles coming from annihilation, it is necessary to study regions where the density of DM is large as this enhances the production of the secondary particles and therefore the flux. For example, the direction of the center of the galaxy is a good place to search for annihilations as particle density in this region is very large and the probability of DM annihilation is larger too.

In the case of the decay of DM, the direction that is considered better to detect these events are the galactic poles as moving away from the galactic center has the advantage of reducing the astrophysical background considerably and the expected flux has less uncertainties as the DM density profile in those areas is better known than the inner dark matter density profile, leading to more robust results. In the end, for any of the two scenarios, the angular size of the detector is a very important feature, as if the telescope is bigger, it can collect more information.

Also, it is expected that DM accumulates around black holes and this may lead to detectable annihilation signals as we expect that DM is distributed in an extremely cuspy way around these objects, allowing them to be bright sources of gamma rays and other annihilation product.

Also, the formation of structures have some important consequences as substructure can have a deep impact on the predicted annihilation signals as the subhalos are denser than the host halo and this enhances the rate of annihilation as it is proportional to the density squared [15]. Also, the decay signal is directly proportional to mass density and therefore, its effect on halo emission profiles from dark matter decay is negligible except when dealing with individual massive objects within a host halo. Very luminous groups can act as individual sources and also, for example in the Milky Way, massive objects as the Sun moving through the galaxy halo can trap gravitationally a sufficiently large amount of DM particles in its center enhancing the probability of annihilation that can produce particles such as neutrinos. The neutrinos can escape from the Sun with a minimum absorption and be detected in many of the large neutrino detectors in the Earth.

Even if detection depends on the local density of DM and the velocity distribution, this involves minimum astrophysical uncertainties compared with other techniques as the annihilation rate is determined by the total number of WIMPS captured along the billions of years and not on properties as the distribution of DM in the galaxy, the magnetic properties of the star or the radiation fields, and it is the reason why to study this approach is very interesting.

One of the main missions of a neutrino telescope is looking for an excess of high energy neutrinos coming from the Sun that will be relate to DM annihilation in its center. Neutrino detectors cannot detect neutrinos directly as they rarely interact with matter and all the neutrino information is obtained by the kinematic information acquire by the not so common collisions between a neutrino and the atoms of the detector. This process are so unsual that the observation of the event generally involve instrumenting a large volume of water or ice. Usually, the product of the interaction is a muon (or a charged lepton in general) but these particles can be also created by cosmic rays and therefore, these type of detectors are buried deeply in the ground to protect it from other background sources as this one. One example of this kind of experiments is the IceCube Neutrino Observatory [16] constructed at the AmundsenScott South Pole Station in Antarctica. Muons are charged particles and if the muon produced by the neutrino-atom interaction inside the medium moves faster than the speed of light in the corresponding medium (ice or water), Cherenkov radiation is produced along the muon path. This light can be detected by the photomultipliers deployed for this purpose in the detector structure.

Current limits from indirect detection are already beginning to constrain the canonical thermal relic annihilation cross section for WIMP dark matter, and the next several years will be a key time as the reach of upcoming experiments is expected to dramatically increase and bring new light to this remarkable DM problem.

2.4.3 Direct detection

Direct detection experiments are a very promising and interesting way to try to probe directly DM interaction in the Milky Way and therefore identify its nature and the idea behind them is really simple to explain [17]. In these experiments, we try to observe and measure the signals produced as the result of the interaction of a DM particle from our own galaxy halo that travelled through the Earth and the matter in our detectors. These signals can be the recoil energy of the nuclei after the scattering, the ionization of the nuclei, an increase in the temperature or we can produce photons or phonons.

We can classify the DM-detector scattering as elastic or inelastic, and spin dependent or spin independent.

In the elastic scattering, the target nucleus interacts with the WIMP as a whole and then we can measure the spectrum of recoil energy of the target. WIMP with masses of $(10 - 1000)\,\mathrm{GeV/c^2}$ will produce nuclear recoils in the range of $(1 - 100)\,\mathrm{keV}$ [18].

For the inelastic scattering the WIMPS interact with the orbital electrons of the target

nucleus and the possible results can be the excitation of these electrons or the ionization of the nucleus. Also, the excitation of the nucleus can happen sometimes but this case is more difficult to study as the background is more complicated to set in this case.

The spin dependent interactions come from the coupling of the DM spin with the spin of the nucleon and in this case, the cross section is proportional to $J(J+1)$. The best limit to date comes from PICO-60, excluding spin-dependant cross sections above 2.5×10^{-41} cm^2 for a WIMP with mass of 25 GeV [19, 20].

For spin independent, the cross section increases with the mass of the nucleus and it dominates over the spin dependent scattering as we use already heavy nucleus in the detectors.

Nowadays, many experiments for direct detection are operating or are in development and thanks to them we have had a significant growth in techniques and technologies that allow us to measure the different types of signals and has caused the rapid progress of this field. Some of these experiments are: Xenon1T [21], PandaX-II [22] and LZ [23] using liquid Xenon; DarkSide-50 [24] that uses liquid Argon; SuperCDMS [25], CDMSlite [26] and CDEX [27] using Germanium; DAMIC [28] using silicon; PICASSO [29] and PICO-60 [30] using Flourine and COUPP [31] using Flourine and Iodine; DAMA [32], KIMS [33] and the future COSINUS [34] using Sodium iodine; CRESST-II [35] using $CaWO_4$ and others.

Many experiments have established strong limits in the interaction cross section of nucleons and DM but experiments keep improving with the hope of making a discovery with time. The most constraining experiments for large DM masses is Xenon1T [21], and for a lower range of masses DarkSide-50 [24] is one of the most constraining for its low velocity threshold. In Figure (2.5), we can see the current limits for spin independent cross section from the most recent experiments.

Detection rates

The main ingredients for the computation of the event rates in direct detection experiments are the local density of DM, the velocity distribution of WIMPS close to the Sun and the WIMP-nucleon cross section [12].

The local density of DM in our solar system is an interesting data. The first estimation was done by J.H. Jean in 1922. For this he analysed the movement of the nearby stars transverse to the galactic plane and concluded that the density of DM should be approximately equal to the density of visible matter as stars, gas and dust. The latest estimation

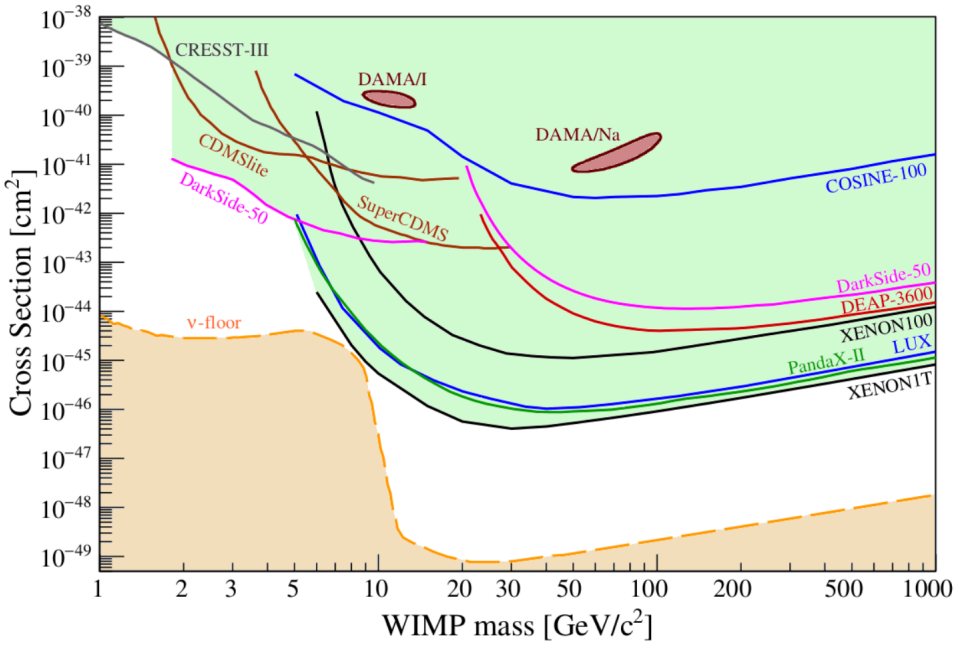

Figure 2.5: Limits on DM-nucleon Spin-independent cross section for the latest direct detection experiments [36].

based on a more detailed model of our galactic system that includes the measurement of the rotation curve for the Milky Way found a similar result [2]

$$\rho_{DM}^{local} = (0.39 \pm 0.03)\,\mathrm{GeV/cm^3}. \tag{2.25}$$

The shape of DM Halo far away from the galactic center is mostly established but the profile in the internal part of the galaxy is not well known. This is the reason why study massive disc galaxies is important as the rotation curves from them can reveal evidence that supports a specific profile for the DM Halo. The observations from the X-ray Observatory Chandra coming from Abell 2029 suggest that the profile is compatible with a cusp profile.

Differential event rate

The differential event rate per unit time per unit recoil energy for DM-nucleon elastic scattering is given [37] by

$$\frac{dR}{dE_R} = \left\langle \frac{\rho_\chi m_T}{\mu_T^2 m_\chi v} \frac{d\sigma}{d\cos\theta} \right\rangle \tag{2.26}$$

where $\langle\rangle$ indicate average over the halo velocity distribution and all the required remaining information come from three different sources. First, the DM density ρ_χ in the solar system and the relative velocity v between dark matter and nucleus come from astrophysics.

Second, the nucleus mass m_T and the reduced mass of the DM-nucleus system μ_T come from detector physics. And finally, the differential scattering cross section with respect to the cosine of the scattering angle θ in the center of mass frame $\frac{d\sigma}{d\cos\theta}$ comes from particle physics and it is given by

$$\frac{d\sigma}{d\cos\theta} = \frac{1}{2j_\chi+1}\frac{1}{2j+1}\sum_s \frac{1}{32\pi}\frac{|\mathcal{M}|^2}{(m_\chi+m_T)^2} \tag{2.27}$$

where j_χ, j are the spins of dark matter and nucleus, respectively, and $\mathcal{M}$ is the scattering amplitude.

Here, we note that $\langle\ \rangle$ is the average over the halo velocity distribution, namely, $\int_{v_{min}=q/(2\mu_T)} d^3v f(v)$ where $f(v)$ is the velocity distribution function and $v_{\rm min}$ is the minimum relative velocity to make the nuclear recoil happen for a given momentum transfer q.

The event rate per unit time per unit recoil energy per detector mass is given [37] by

$$\frac{dR_D}{dE_R} = N_T \cdot \frac{\rho_\chi m_T}{32\pi m_\chi^3 m_N^2} \cdot \left\langle \frac{1}{v}\sum_{i,j}\sum_{N,N'=n,p} c_i^{(N)} c_j^{(N')} F_{ij}^{(N,N')}(v^2,q^2) \right\rangle \tag{2.28}$$

where N_T is the number of target nuclei in a given detector, $c_i^{(N)}$ are the coefficients of non-relativistic nucleon operators, $\mathcal{O}_i^{\rm NR}$, in the effective Lagrangian, and $F_{ij}^{(N,N')}(v^2,q^2)$ are the nucleon form factors, with symmetric property under $(i,N) \leftrightarrow (j,N')$. As we can see, this quantity depends on the detector material and mass.

Other thing that we have to keep in mind for the rate computations is the annual modulation of the signals due to the Earth annual rotation around the Sun and at the same time, the relative movement of the sun through the DM halo [38], thus, the velocity distribution function must contain this information [39]. The observation of this modulation would be a smocking-gun signature on DM experiments. Two experiments report annual modulation in the signals, DAMA [40] and CoGeNT [41]. As we can note, in some part of the year the orbital velocity is parallel to the WIMP wind and this will increase the apparent WIMP velocity and therefore the rate and in a different season, it is anti-parallel and this will have the opposite effect. Diurnal direction modulation due to Earth rotation about its axis can have an effect also.

Chapter 3

Gravity-mediated or Composite Dark Matter

Until now, all the evidence of the existence of dark matter is due to its gravitational effect on other objects and therefore the only thing that we know for sure about its behaviour is that DM interacts gravitationally with the SM matter. This chapter is a small review of the basic idea in the work done by Hyun Min Lee, Myeonghun Park and Veronica Sanz [5,42] about a model called Gravity Mediated Dark Matter where the gravity mediators are the bridge between the visible and invisible world.

3.1 Model with Warped Extra Dimensions

The motivation to introduce extra dimensions has been changing in time since the first publication of Kaluza in 1984 [43]. In this first work, the main idea was to deal with the problem of unification of gravity and electromagnetism in 4+1 dimensions. This work came after the theoretical aspects of the General Relativity (GR) were well established and pointed out how the forces known at that time can be described in a unified way if one spatial extra dimension is splitted. With the posterior work of Klein [44], who introduce the concept of an extra dimension, this idea is related with an associated compactification scale and it was the the starting point to generate a set of theories called Kaluza-Klein models. The consequences of these models are the introduction of a scheme of components corresponding to a spin-2 $g_{\mu\nu}$, spin-1 A_μ and spin-0 $\bar{g}_{55}$ fields transforming in a 4 dimensional Lorentz group. At low energies, the Kaluza-Klein theory describes 4D gravity, a $U(1)$ gauge theory and a real scalar field with dilaton couplings that can be interpreted as oscillations that generate the radion field (For a review see [45] and references

therein). Although some efforts have been done to generate non-Abelian gauge theories using exotic properties of extra dimensions, up today there is not a satisfactory model that can generate the SM gauge group with its chiral properties using only a geometric structure. Nevertheless it is important to mention that the introduction of a very large (of the order fo milimeters) compactified space can eliminate the large hierarchy between the electroweak scale and the fundamental scale of gravity. Some authors [46–48] had proposed an interesting idea, which resides in the introduction of three-branes allowing gravity to propagate only on the extra dimensions. Although from the phenomenological point of view is difficult to fit into the observations, this propousal is one of the main motivations to pursuing alternative models as the one where gauge and fermions fields are allowed to propagate in the extra dimensions. A interesting model of this kind can bee seen in [49].

In the search of more realistic versions of extra dimensions models, we can distinguish two elements. On one side, singularities of the geometric structures called branes and on the other hand, fields that propagates on this structures. Thus a model is defined setting the localization of fields in these different structures that compose the extra dimensions. Conventionally, this imply that extra dimensions with significant curvature allow that only some fields could propagate in the bulk . For the purpose of this thesis, we mention only two cases: (i) when only gravity propagates on the bulk as the Randall-Sundrum (RS) model [50, 51] and (ii) the case when gravity and additional field mediators propagate in the bulk . Both cases have the advantage that they solve the hierarchy problem without large extra dimensions introducing a factor into the metric that changes abruptly with the extra dimension. In the particular case of the RS model, an orbifold S^1/Z_2 is introduced and there are two branes on the opposite sides of a extra dimension. In this model a cosmological constant in the bulk serves as the source of the gravity. This model is characterized by the metric

$$ds^2 = e^{-2kr_c\phi}\eta_{\mu\nu}dx^\mu dx^\nu + r_c^2 d\phi^2 \tag{3.1}$$

As a consequence, the fields that are confined in the brane have a physical mass regulated by a decreasing exponential factor of the form $m = m_0 e^{-kr_c\pi}$. Fixing the value of kr_c, the weak scale can be generated from the effective Planck scale of the model. Also, the Kaluza-Klein gravitational modes have mass splitting and couplings of the order of TeV. In order to avoid fine tunning for kr_c, the introduction of a scalar field that exist in the bulk action was proposed in [52]. Such field have two characteristics, it takes vacuum expectation values (VEV's) on the branes and generate a potential in the action that have

a minimum at

$$kr_c = \left(\frac{4}{\pi}\right)\frac{k^2}{m^2}\ln\left(\frac{v_h}{v_v}\right). \tag{3.2}$$

Here, v_h and v_v are the VEV's in the corresponding branes $\phi = 0$ (hidden) and $\phi = \pi$ (visible) respectively. Taking the condition $v_h << v_v$ and $k^2/m^2 \sim 10$, reasonable values for the weak scale can be obtained. In general, the RS model metric can be written as [53]

$$ds^2 = e^{-2k|\phi|T(z)}g_{\mu\nu}dx^\mu dx^\nu - T^2(z)d\phi^2, \tag{3.3}$$

where $g_{\mu\nu}(z)$ and $T(z)$ are the 4-dimensional graviton and radion respectively. In order to obtain a suitable value of kr_c to solve the hierarchy problem, the mass of the radion must be of the order of TeV. This makes the model very interesting from the phenomenological point of view and this will be the starting point of the model described below.

To face the problem of explain the relic abundance of DM, has been proposed many models of weak interactions between SM particles and DM. We can mention the Supersymmetric models [54–56] and Universal Extra dimensional models [57–61]. In the context of the extensions of the SM, some models assume the interaction of the DM only through a particle called a portal. The nature of this interacting particle that serves as a bridge between SM fields and DM is determined by the symmetries of the SM extensions. we can mention two important examples of portals: the Higgs portal and the dark photon.

In the case of Higgs portal is stablished by the extension of the scalar and Yukawa sector of SM though the introduction of SU(2) singlets [62, 63] or doublets in the context of a hidden gauge sector as in [64–68] to mention some examples.

Nevertheless, up today, the only known interaction between baryonic matter and DM is gravity. Based in this observation is assume a realistic model that naturally contain exclusively gravitational interactions. It worth to mention that term natural is not related with the naturalness argument introduce in some extended theories to fix the scale o New Physics effects as in Supersymmetry models. In this work is stated that natural models to describe the DM matter interaction are those that contain only gravity-mediators. The particular model used in this thesis, produce thermally the correct abundance of DM in the Universe in contrast with those models that introduce heavy DM particles or WIMPZILAS to produce non-thermally relic abundance [69–72]. The typical gravity-mediators of models mentioned above are the radion and the massive graviton that arise from warped extra dimensions. Hello Let start considering the following class of five-dimensional metrics,

$$ds^2 = w(z)^2\left(\eta_{\mu\nu}dx_\mu dx_\nu - dz^2\right), \tag{3.4}$$

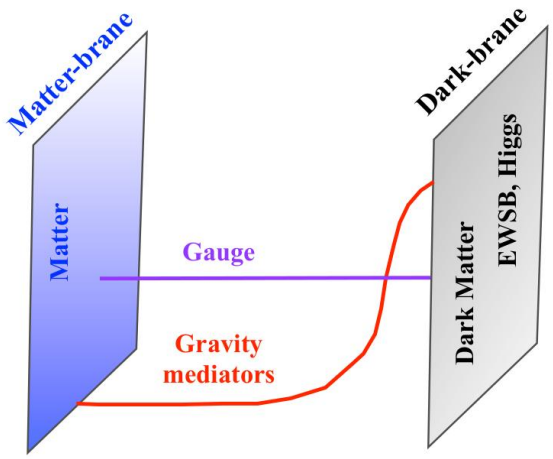

Figure 3.1: Set up for the GMDM model with extra dimensions [5].

where z is the coordinate in the 5th dimension and w(z) is a smooth, decreasing or constant function of this coordinate. This is a generalization of the the metric (3.1) where w(z) = 1/(kz) and k is the curvature of the five-dimensional (5D) space-time. Here we are considering also warped extra-dimensions as in Anti-deSitter (AdS) models.

The fifth dimension is compactified on an interval $z \in [z_0, z_1]$, and four-dimensional (4D) branes are located at both ends of the extra-dimension. The brane located at z_0 is called the Matter-brane and contain all SM particles. In the brane at z_1 is located the Higgs and the DM particles, we call this brane the Dark-brane. A visual description of this model taken from [5] is shown in Fig. 3.1

Fields located on branes become truly 4D fields but gravity and its excitations do necessarily propagate in the full 5D space-time. In this set-up, the fields associated to the Higgs and DM fieldsare restricted to the Dark-brane because its role in the electroweak symmetry breaking. An example of this idea could be a composite Higgs sector [73–77] where DM could be part of the pseudo-Goldstone sector and it is protected by a left-over symmetry.

However, in this model DM is considered scalar, vector and fermionic particles and it will be described by its general properties: DM is a singlet under the SM with a mass at the electroweak scale and it is stable due to a quantum number conserved by the Dark-brane dynamics.

As a singlet of the SM, DM interacts exclusively through gravitational interactions. The interaction of the massless graviton with any field is suppressed by M_{Pl}, and the leading interactions come from exchanging other gravitational fields, specifically gravity

mediators as the radion and the Kaluza-Klein (KK) massive gravitons.

Gravity and gauge fields live in the bulk of the extra-dimensions, it has fully 5D dynamics, but their localization is different. Massless gauge bosons are de-localized in the bulk, with a flat profile and gravity mediators (KK-graviton and radion) are peaked towards the Dark-brane as a result of the warping. And the SM matter fields are localized on the Matter-brane.

The graviton and the radion are described by the tensor and scalar fluctuations of the metric, introduced as an expansion in 3.4

$$ds^2 = w(z)^2 \left(e^{-2r}(\eta_{\mu\nu} + G_{\mu\nu})dx^\mu dx^\nu - (1+2r)^2 dz^2\right). \tag{3.5}$$

where $G_{\mu\nu}$ and r are 5D fields propagating in the extra-dimension. The expression (3.5) was chosen to solve the hierarchy problem with the mechanism of the RS model and also to introduce an *ad. hoc.* propagation in the bulk of the gravity-mediators.

We focus on the Kaluza-Klein (KK) resonance of the fields, including the effect of the whole tower. As usual we express

$$G^n_{\mu\nu}(x,z) = G^n_{\mu\nu}(x) f^n_G(z) \tag{3.6}$$

$$r^n(x,z) = r^n(x) f^n_r(z) \tag{3.7}$$

for the nth KK resonance of the graviton and nth resonance of the radion respectively. In the following we adopt the notation without the n index for this resonances treating this resonances in a generic way.

We consider the general interactions of a KK graviton $G_{\mu\nu}$ and the radion r to a pair of particles. The interaction arises by expanding the metric in 3.5 at linear order in r and $G_{\mu\nu}$ in the action

$$S \supset \int d^d x \sqrt{-g}\mathcal{L} \supset \int d^d x \sqrt{-g} w(z)^2 \left(2rT - G_{\mu\nu}T^{\mu\nu}\right) \tag{3.8}$$

Inserting the bulk profile of the fields and integrating out the extra-dimension, we obtain the 4D effective Lagrangian at dimension-five,

$$\mathcal{L}_{KK} = -\frac{c_i^G}{\Lambda} G_{\mu\nu} T_i^{\mu\nu} + \frac{c_i^r}{\sqrt{6}\Lambda} r T_i, \tag{3.9}$$

where $T_i^{\mu\nu}$ is the energy-momentum tensor of species i and T_i is its trace. Λ is the compactification scale, related to the position of the Dark brane, $\Lambda = 1/z_{Dark} \backsim TeV$. The coefficients $c_i^{r,G}$ arise by dimensional reduction from the 5D theory to the 4D low-energy effective theory and are given by

$$c_i^G \propto \int dz f_G(z) f_i(z)^2 \tag{3.10}$$

$$c_i^r \propto \int dz f_r(z) f_i(z)^2 \tag{3.11}$$

where we have use the generic expressions (3.6) and $f_i(z)^2 \propto \delta(z - z')$ is the restriction on the i field lying on the brane at z. As was mentioned before, the gauge fields de-localized in the bulk implies $f_i \propto$ constant.

The KK gravitons $G_{\mu\nu}$ satisfies traceless and transverse conditions, $G^\mu_\mu = \partial_\mu G^{\mu\nu} = 0$, which leads to a rather generic interactions,

$$\begin{aligned}\mathcal{L}_{KK} &= -\frac{1}{\Lambda} G^{\mu\nu} \left[T^{DM}_{\mu\nu} - c_V^G F_{\mu\lambda} F^\lambda_\nu + c_\psi^G \left(\frac{i}{4} \bar{\psi} (\gamma_\mu D_\nu + \gamma_\nu D_\mu)\psi - \frac{i}{4} (D_\mu \bar{\psi} \gamma_\nu + D_\nu \bar{\psi} \gamma_\mu)\psi \right) \right] \\ &\quad -\frac{1}{\Lambda} G^{\mu\nu} c_H^G \left(D_\mu H^\dagger D_\nu H + D_\nu H^\dagger D_\mu H \right)\end{aligned} \tag{3.12}$$

with the traceless part of the energy-momentum tensor for DM given by

$$T^{DM}_{\mu\nu} = c_X^G (-X_{\mu\lambda} X^\lambda_\nu + m_X^2 X_\mu X_\nu), \qquad \text{vector DM,} \tag{3.13}$$

$$T^{DM}_{\mu\nu} = c_\chi^G \left(\frac{i}{4} \bar{\chi} (\gamma_\mu \partial_\nu + \gamma_\nu \partial_\mu)\chi - \frac{i}{4} (\partial_\mu \bar{\chi} \gamma_\nu + \partial_\nu \bar{\chi} \gamma_\mu)\chi \right), \qquad \text{fermion DM} \tag{3.14}$$

$$T^{DM}_{\mu\nu} = c_S^G \partial_\mu S \partial_\nu S, \qquad \text{scalar DM} \tag{3.15}$$

Here, the c's are KK graviton couplings which are determined by the overlap between the wave functions of the KK graviton and fields in extra dimensions.

The massless gauge fields do not contribute to the trace of the energy-momentum tensor at the tree level, but they generate trace anomalies at the loop level that are highly suppressed.

Regarding the masses of the KK-graviton, it is $m_G \lesssim \Lambda$ and the exact relation depends on the metric. In AdS models the mass of the KK-graviton is related to k, Planck mass M_{Pl} and Λ by

$$m_G = \frac{k}{M_P} x_G \Lambda, \tag{3.16}$$

where one expects $k \lesssim M_{Pl}$. In other metrics, the relation between the curvature and the graviton mass would be different but, generally speaking, one expects that a healthy theory satisfies $m_G \lesssim \Lambda$ to make consistent the gravity-mediator with the electroweak scale.

On the other hand, the radion mass is a model-dependent parameter, related to the mechanism of stabilization of the extra-dimension. In absence of stabilization the radion is exactly massless [78, 79].

Chapter 4

Dark Matter Direct Detection from model with spin-2 mediators

We consider a massive spin-2 particle as the mediator that couples to dark matter and the SM particles. In this case we consider that the spin of DM is arbitrary, this means, we consider the cases where DM are scalars, fermions and vector particles. The coupling of the different type of particles to the spin-2 resonance is through the energy-momentum tensor [5, 42, 80–82]. In this case, after integrating out the mediator, we can identify the effective interactions between dark matter and the SM quarks up to dimension-8 and match them to the gravitational form factors for nucleons beyond a zero momentum transfer. Using this we can study direct detection, production of DM in colliders and relic density.

4.0.1 Effective interactions between dark matter and quarks

As it was mentioned before, the spin-2 mediator couples to the SM and DM particles through the energy-momentum tensor, as follows [5, 42, 80, 81],

$$\mathcal{L}_{\rm int} = -\frac{c_{\rm SM}}{\Lambda}\mathcal{G}^{\mu\nu}T^{\rm SM}_{\mu\nu} - \frac{c_{\rm DM}}{\Lambda}\mathcal{G}^{\mu\nu}T^{\rm DM}_{\mu\nu}. \tag{4.1}$$

In this case, the mediator couplings for the SM particles can vary, depending on the location in the extra dimension [5, 42]. Then, the tree-level scattering amplitude between DM and SM particles through the spin-2 mediator is given by

$$\mathcal{M} = -\frac{c_{\rm DM}c_{\rm SM}}{\Lambda^2}\frac{i}{q^2 - m_G^2}T^{\rm DM}_{\mu\nu}(q)\mathcal{P}^{\mu\nu,\alpha\beta}(q)T^{\rm SM}_{\alpha\beta}(-q) \tag{4.2}$$

where q is the 4-momentum transfer between dark matter and the SM particles and the tensor structure for the massive spin-2 propagator is given by

$$\mathcal{P}_{\mu\nu,\alpha\beta}(q) = \frac{1}{2}\Big(G_{\mu\alpha}G_{\nu\beta} + G_{\nu\alpha}G_{\mu\beta} - \frac{2}{3}G_{\mu\nu}G_{\alpha\beta}\Big) \tag{4.3}$$

with

$$G_{\mu\nu} \equiv \eta_{\mu\nu} - \frac{q_\mu q_\nu}{m_G^2}. \tag{4.4}$$

We note that the sum of the spin-2 mediator polarizations is given by

$$\sum_s \epsilon_{\mu\nu}(q,s)\epsilon_{\alpha\beta}(q,s) = P_{\mu\mu,\alpha\beta}(q). \tag{4.5}$$

The tensor $P_{\mu\mu,\alpha\beta}$ satisfies traceless and transverse conditions for on-shell spin-2 mediator, such as $\eta^{\alpha\beta}P_{\mu\mu,\alpha\beta}(q) = 0$ and $q^\alpha P_{\mu\mu,\alpha\beta}(q) = 0$ [5].

Due to energy-momentum conservation

$$q_\mu T^{\mu\nu} = 0 \tag{4.6}$$

we can rewrite the scattering amplitude replacing $G_{\mu\nu}$ by $\eta_{\mu\nu}$ and then we can divide the amplitude into trace and traceless parts of energy-momentum tensor, as follows,

$$\begin{aligned}\mathcal{M} &= \frac{ic_{\rm DM}c_{\rm SM}}{2m_G^2\Lambda^2}\left(2T^{\rm DM}_{\mu\nu}T^{{\rm SM},\mu\nu} - \frac{2}{3}T^{\rm DM}T^{\rm SM}\right)\\ &= \frac{ic_{\rm DM}c_{\rm SM}}{2m_G^2\Lambda^2}\left(2\tilde{T}^{\rm DM}_{\mu\nu}\tilde{T}^{{\rm SM},\mu\nu} - \frac{1}{6}T^{\rm DM}T^{\rm SM}\right)\end{aligned} \tag{4.7}$$

where $\tilde{T}^{\rm SM(DM)}_{\mu\nu}$ is the traceless part of energy-momentum tensor given by $\tilde{T}^{\rm SM(DM)}_{\mu\nu} = T^{\rm SM(DM)}_{\mu\nu} - \frac{1}{4}\eta_{\mu\nu}T^{\rm SM(DM)}$ with $T^{\rm SM(DM)}$ being the trace of energy-momentum tensor.

The energy momentum tensor for the SM quarks denoted by ψ [5] is, in momentum space,

$$T^{\psi}_{\mu\nu} = -\frac{1}{4}\bar{u}_\psi(p_2)\Big(\gamma_\mu(p_{1\nu}+p_{2\nu}) + \gamma_\nu(p_{1\mu}+p_{2\mu}) - 2\eta_{\mu\nu}(\not{p}_1 + \not{p}_2 - 2m_\psi)\Big)u_\psi(p_1) \tag{4.8}$$

where $u_\psi(p)$ is the Dirac spinor for ψ. Here, the SM fermion is incoming into the vertex with momentum p_1 and is outgoing from the vertex with momentum p_2. Then, the trace of the energy-momentum tensor for ψ is given by

$$T^{\psi} = -\frac{1}{4}\bar{u}_\psi(p_2)\Big(-6(\not{p}_1 + \not{p}_2) + 16m_\psi\Big)u_\psi(p_1). \tag{4.9}$$

The traceless part of the energy-momentum tensor for ψ is given by

$$\tilde{T}^{\psi}_{\mu\nu} = -\frac{1}{4}\bar{u}_\psi(p_2)\Big(\gamma_\mu(p_{1\nu}+p_{2\nu}) + \gamma_\nu(p_{1\mu}+p_{2\mu}) - \frac{1}{2}\eta_{\mu\nu}(\not{p}_1 + \not{p}_2)\Big)u_\psi(p_1). \tag{4.10}$$

4.0.2 Gravitational form factors for nucleons

So far, all the study has been done considering the interaction of DM with quarks but for the study of DM direct detection is necessary to consider the interaction with the nucleons instead. To go from quarks to nucleons we need to do the match of the terms in the energy-momentum tensor to the nuclear matrix elements. In the case of the trace part (4.9), we can do this match as follows,

$$\langle N(p_2)|T^{\psi}|N(p_1)\rangle = -F_S(q^2) m_N \bar{u}_N(p_2) u_N(p_1) \tag{4.11}$$

where $F_S(q^2)$ is the form factor for the scalar current, given at $q = 0$ by $F_S(0) = f^N_{T\psi}$ [83]. Here, we note that f^N_{Tq} denote the mass fractions of light quarks in a nucleon. The values for $f^N_{T\psi}$ considered in this study are shown in Table 4.1.

On the other hand, the most general structure of the energy-momentum tensor (4.8) is matched to the nuclear matrix elements writing it in terms of three gravitational form factors $A(q^2), B(q^2), C(q^2)$ [84–86],

$$\begin{aligned}\langle N(p_2)|T^{\psi}_{\mu\nu}|N(p_1)\rangle &= \bar{u}_N(p_2)\Big(A(q^2)\gamma_{(\mu}p_{\nu)} + B(q^2)\frac{1}{2m_N} ip_{(\mu}\sigma_{\nu)\lambda}q^{\lambda} \\ &\quad + C(q^2)\frac{1}{m_N}(q_\mu q_\nu - \eta_{\mu\nu}q^2)\Big)u_N(p_1) \\ &= \bar{u}_N(p_2)\Big(\frac{2}{m_N}A(q^2)p_\mu p_\nu + (A(q^2)+B(q^2))\frac{1}{2m_N} ip_{(\mu}\sigma_{\nu)\lambda}q^{\lambda} \\ &\quad + C(q^2)\frac{1}{m_N}(q_\mu q_\nu - \eta_{\mu\nu}q^2)\Big)u_N(p_1)\end{aligned} \tag{4.12}$$

where $p_\mu = \frac{1}{2}(p_1 + p_2)$ and $q = p_2 - p_1$ and $(\,)$ means the symmetrization of indices. Using the Gordon identity to rewrite the previous expresion as follow,

$$\begin{aligned}\langle N(p_2)|T^{\psi}_{\mu\nu}|N(p_1)\rangle &= \bar{u}_N(p_2)\Big(\frac{2}{m_N}A(q^2)p_\mu p_\nu + (A(q^2)+B(q^2))\frac{1}{2m_N} ip_{(\mu}\sigma_{\nu)\lambda}q^{\lambda} \\ &\quad + C(q^2)\frac{1}{m_N}(q_\mu q_\nu - \eta_{\mu\nu}q^2)\Big)u_N(p_1)\end{aligned} \tag{4.13}$$

we note that the second term is the anomalous gravitational magnetic moment operator. As it is shown in Ref. [84–86], one can check that the form factors $A(q^2), B(q^2)$ and $C(q^2)$ are the only ones that are consistent with Lorentz invariance, $q_\mu T^{\psi,\mu\nu} = 0$, and CP symmetry.

Now, we want to find the matching for the traceless part. For this, let's start considering the energy-momentum tensor for on-shell nucleons,

$$\begin{aligned}T^N_{\mu\nu} &= -\frac{1}{2}\bar{u}_N(p_2)\gamma_{(\mu}p_{\nu)}u_N(p_1) \\ &= -\frac{1}{2}\bar{u}_N(p_2)\Big(\frac{2}{m_N}p_\mu p_\nu + \frac{1}{2m_N} ip_{(\mu}\sigma_{\nu)\lambda}q^{\lambda}\Big)u_N(p_1).\end{aligned} \tag{4.14}$$

With this expression, we can rewrite the above nuclear matrix elements in equation (4.13) as

$$\begin{aligned}\langle N(p_2)|T^{\psi}_{\mu\nu}|N(p_1)\rangle &= -2(A(q^2)+B(q^2))T^{N}_{\mu\nu} \\ &+\frac{1}{m_N}\,\bar{u}_N(p_2)\Big(-2B(q^2)p_\mu p_\nu + C(q^2)(q_\mu q_\nu - \eta_{\mu\nu}q^2)\Big)u_N(p_1)\end{aligned} \tag{4.15}$$

where $T^N_{\mu\nu}$ is the energy-momentum tensor for nucleons. Then, using equation (4.16) and its trace, we obtain the nuclear matrix elements for the traceless part of the energy-momentum tensor as

$$\begin{aligned}\langle N(p_2)|\tilde{T}^{\psi}_{\mu\nu}|N(p_1)\rangle &= -2(A(q^2)+B(q^2))\tilde{T}^{N}_{\mu\nu} + \frac{1}{m_N}\,\bar{u}_N(p_2)\Big[-2B(q^2)\Big(p_\mu p_\nu - \frac{1}{4}g_{\mu\nu}p^2\Big) \\ &+C(q^2)\Big(q_\mu q_\nu - \frac{1}{4}\eta_{\mu\nu}q^2\Big)\Big]u_N(p_1).\end{aligned} \tag{4.16}$$

Now, for nucleons with zero momentum transfer, the above result (4.16) [87–89] becomes

$$\langle N(p)|\tilde{T}^{\psi}_{\mu\nu}|N(p)\rangle = -\frac{1}{m_N}F_T(0)\Big(p_\mu p_\nu - \frac{1}{4}m_N^2 g_{\mu\nu}\Big)\bar{u}_N(p)u_N(p) \tag{4.17}$$

where the form factor for the twist-2 quark operator is given by $F_T(0) \equiv -2A(0) = \psi(2)+\bar{\psi}(2)$ and $\psi(2)+\bar{\psi}(2)$ are the second moments of the parton distribution functions (PDFs) of the corresponding particle. Also, $B(q^2), C(q^2)$ remain unfixed due to lack of the extra information on the form factors for a nonzero momentum transfer. The second moments of PDFs in a proton have scale dependence, so we evaluate them at the scale $\mu = m_Z$ because the effective couplings are matched at the scale of the mediator particle [88]. The values are shown in Table 4.2.

$f^N_{T\psi}$	Value
f^p_{Tu}	0.023
f^p_{Td}	0.032
f^p_{Ts}	0.020
f^n_{Tu}	0.017
f^n_{Td}	0.041
f^n_{Ts}	0.020

Table 4.1: The mass fractions for protons and neutrons [88]

The same results can be obtain in a holographic description of QCD with the hard-wall or soft-wall model in a five-dimensional Anti-de Sitter (AdS) spacetime (to read an

Twist-2	Value
$u(2)$	0.22
$\bar{u}(2)$	0.034
$d(2)$	0.11
$\bar{d}(2)$	0.036
$s(2) = \bar{s}(2)$	0.026
$c(2) = \bar{c}(2)$	0.019
$b(2) = \bar{b}(2)$	0.012

Table 4.2: The second moments of PDFs calculated at the scale $\mu = m_Z$ using the CTEQ parton distribution [88].

introduction to this topic go to reference [86]) where the gravitational form factors can be described by the three-point correlation function between the zero-mode graviton and a fermion in the bulk on the boundary of the AdS spacetime. In this case, the relation between the gravitational form factors is given by $A(q^2) \neq 0$ and $B(q^2) = C(q^2) = 0$ even for a nonzero momentum transfer [86]. This allows us to do the matching of the quark operators in equation (4.16) to the nucleon form factors with a general momentum transfer by the overall form factor $F_T(q^2)$ as follows,

$$\langle N(p_2)|\tilde{T}^{\psi}_{\mu\nu}|N(p_1)\rangle = F_T(q^2)\tilde{T}^{N}_{\mu\nu} \tag{4.18}$$

with $F_T(q^2) \equiv -2A(q^2)$. This form factor has been explicitly computed in a holographic set-up with a *soft wall* model. This would be the dual of theories with a conformal UV limit and a softly broken symmetry at low energies. The breaking is then spontaneous and the features of the soft wall allow for switching on an non-zero expectation value for an operator with finite canonical dimension or a non-AdS background mass of the dual fields as it is explained in Reference [90].

In this context, Ref. [86] finds an explicit form of the form factor, which decreases with q^2 as shown in Fig. 4.1, and admits an expansion near $q^2 \simeq 0$ as follows

$$F_T(q^2) \simeq -2(1 - q^2/(0.55\ \text{GeV})^2 \ldots). \tag{4.19}$$

For simplicity, we assume that this is the case and also we take $F_T(q^2) \approx F_T(0)$.

Further improvements in the analysis could be done by simultaneously expanding the form factor coupling $F_T(q^2)$ and following the standard procedure of non-relativistic expansion described in the next Section.

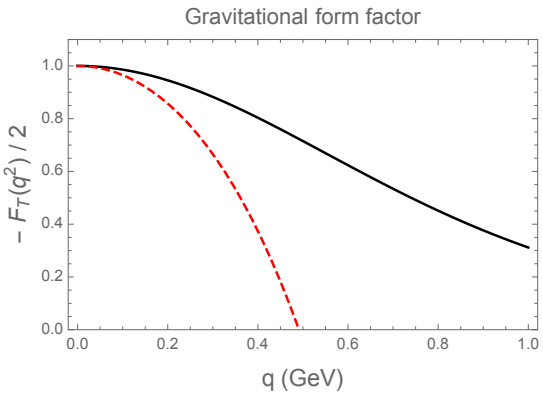

Figure 4.1: Gravitational form factor $-F_T(q^2)/2$ as a function of the momentum transfer q in GeV. The black line corresponds to the exact expression obtained in Ref. [86] and the same input parameters. The red-dashed line corresponds to the quadratic approximation.

4.1 Effective operators for DM-nucleon scattering

In this section, we discuss the effective Lagrangian for the elastic scattering between fermion and scalar dark matter and nucleons due to the spin-2 mediator.

4.1.1 Fermion dark matter

In momentum space, the energy-momentum tensor for a fermion DM χ is,

$$T^{\chi}_{\mu\nu} = -\frac{1}{4}\bar{u}_{\chi}(k_2)\Big(\gamma_{\mu}(k_{1\nu}+k_{2\nu}) + \gamma_{\nu}(k_{1\mu}+k_{2\mu}) - 2\eta_{\mu\nu}(\not{k}_1+\not{k}_2-2m_{\chi})\Big)u_{\chi}(k_1) \quad (4.20)$$

where the fermion DM particle is incoming into the vertex with momentum k_1 and it is outgoing from the vertex with momentum k_2. We separate this tensor in the trace and traceless parts. The trace is given by

$$T^{\chi} = -\frac{1}{4}\bar{u}_{\chi}(k_2)\Big(-6(\not{k}_1+\not{k}_2)+16m_{\chi}\Big)u_{\chi}(k_1). \quad (4.21)$$

And the traceless part is given by

$$\tilde{T}^{\chi}_{\mu\nu} = -\frac{1}{4}\bar{u}_{\chi}(k_2)\Big(\gamma_{\mu}(k_{1\nu}+k_{2\nu}) + \gamma_{\nu}(k_{1\mu}+k_{2\mu}) - \frac{1}{2}\eta_{\mu\nu}(\not{k}_1+\not{k}_2)\Big)u_{\chi}(k_1). \quad (4.22)$$

We consider the elastic scattering between the DM fermion and the nucleon. In this case, the nucleon is incoming into the vertex with momentum p_1 and it is outgoing with momentum p_2.

From equations (4.22) and (4.18), the relevant effective interactions for the traceless

parts are

$$\begin{aligned}16\tilde{T}^{\chi}_{\mu\nu}\langle N(p_2)|\tilde{T}^{\psi,\mu\nu}|N(p_1)\rangle &= F_T\Big[(2(p_1+p_2)\cdot(k_1+k_2))(\bar{u}_\chi(k_2)\gamma_\mu u_\chi(k_1))(\bar{u}_N(p_2)\gamma^\mu u_N(p_1))\\ &-(\bar{u}_\chi(k_2)(\not{k}_1+\not{k}_2)u_\chi(k_1))(\bar{u}_N(p_2)(\not{p}_1+\not{p}_2)u_N(p_1))\\ &+2(\bar{u}_\chi(k_2)(\not{p}_1+\not{p}_2)u_\chi(k_1))(\bar{u}_N(p_2)(\not{k}_1+\not{k}_2)u_N(p_1))\Big]\end{aligned} \tag{4.23}$$

Using the Dirac equation $\not{p}u_N(p) = m_N u_N(p)$ we get

$$\begin{aligned}16\tilde{T}^{\chi}_{\mu\nu}\langle N(p_2)|\tilde{T}^{\psi,\mu\nu}|N(p_1)\rangle &= F_T\Big[(2(p_1+p_2)\cdot(k_1+k_2))(\bar{u}_\chi(k_2)\gamma_\mu u_\chi(k_1))(\bar{u}_N(p_2)\gamma^\mu u_N(p_1))\\ &-4m_\chi m_N(\bar{u}_\chi(k_2)u_\chi(k_1))(\bar{u}_N(p_2)u_N(p_1))\\ &+2(\bar{u}_\chi(k_2)(\not{p}_1+\not{p}_2)u_\chi(k_1))(\bar{u}_N(p_2)(\not{k}_1+\not{k}_2)u_N(p_1))\Big]\end{aligned} \tag{4.24}$$

Using Gordon identities,

$$\bar{u}_\chi(k_2)\gamma^\mu u_\chi(k_1) = \frac{1}{2m_\chi}\bar{u}_\chi(k_2)\Big((k_1+k_2)^\mu - i\sigma^{\mu\rho}q_\rho\Big)u_\chi(k_1), \tag{4.25}$$

$$\bar{u}_N(p_2)\gamma^\nu u_N(p_1) = \frac{1}{2m_N}\bar{u}_N(p_2)\Big((p_1+p_2)^\nu + i\sigma^{\nu\lambda}q_\lambda\Big)u_N(p_1), \tag{4.26}$$

we can rewrite the vector operators in terms of scalar and tensor operators and obtain

$$\begin{aligned}16\tilde{T}^{\chi}_{\mu\nu}\langle N(p_2)|\tilde{T}^{\psi,\mu\nu}|N(p_1)\rangle &= F_T\Bigg[\frac{(P\cdot K)}{2m_\chi m_N}\Big((K\cdot P)(\bar{u}_\chi(k_2)u_\chi(k_1))(\bar{u}_N(p_2)u_N(p_1))\\ &+(\bar{u}_\chi(k_2)u_\chi(k_1))(K_\nu\bar{u}_N(p_2)i\sigma^{\nu\lambda}q_\lambda u_N(p_1))\\ &-(P_\mu\bar{u}_\chi(k_2)i\sigma^{\mu\rho}q_\rho u_\chi(k_1))(\bar{u}_N(p_2)u_N(p_1))\\ &-(\bar{u}_\chi(k_2)i\sigma^{\mu\rho}q_\rho u_\chi(k_1))(\bar{u}_N(p_2)i\sigma_{\mu\lambda}q^\lambda u_N(p_1))\Big)\\ &-4m_\chi m_N(\bar{u}_\chi(k_2)u_\chi(k_1))(\bar{u}_N(p_2)u_N(p_1))\\ &+\frac{1}{2m_\chi m_N}\Big((K\cdot P)^2(\bar{u}_\chi(k_2)u_\chi(k_1))(\bar{u}_N(p_2)u_N(p_1))\\ &-(P_\mu\bar{u}_\chi(k_2)i\sigma^{\mu\rho}q_\rho u_\chi(k_1))(K_\nu\bar{u}_N(p_2)i\sigma^{\nu\lambda}q_\lambda u_N(p_1))\\ &+(K\cdot P)(\bar{u}_\chi(k_2)u_\chi(k_1))(K_\nu\bar{u}_N(p_2)i\sigma^{\nu\lambda}q_\lambda u_N(p_1))\\ &-(K\cdot P)(P_\mu\bar{u}_\chi(k_2)i\sigma^{\mu\rho}q_\rho u_\chi(k_1))(\bar{u}_N(p_2)u_N(p_1))\Big)\Bigg]\end{aligned} \tag{4.27}$$

where $P^\mu \equiv (p_1+p_2)^\mu$, $K^\mu \equiv (k_1+k_2)^\mu$ and $q^\mu \equiv (k_1-k_2)^\mu = (p_2-p_1)^\mu$. Using $2p_1\cdot k_1 = s - m_N^2 - m_\chi^2 = 2p_2\cdot k_2$ and $2p_1\cdot k_2 = -u + m_N^2 + m_\chi^2 = 2p_2\cdot k_1$ for nucleon momenta, we note the approximate formula,

$$P\cdot K = (p_1+p_2)\cdot(k_1+k_2) = s - u \simeq 4m_\chi m_N. \tag{4.28}$$

where use is made of $s \simeq (m_\chi + m_N)^2$ and $u \simeq (m_\chi - m_N)^2$ in the non-relativistic limit. The above nucleon operators can be matched to non-relativistic nucleon operators as in Ref. [37], with the exception, the operator in the 7th line in equation (4.27), which is suppressed for a small momentum transfer as will be shown later.

From equations (4.21) and (4.11), the effective interactions for trace parts are

$$T^\chi \langle N(p_2)|T^\psi|N(p_1)\rangle = m_\chi m_N F_S(\bar{u}_\chi(k_2)u_\chi(k_1))(\bar{u}_N(p_2)u_N(p_1)). \tag{4.29}$$

Thus, the trace parts contain only scalar-scalar operators.

Consequently, from equations (4.27) and (4.29), we get the scattering amplitude between fermion dark matter and nucleon as follows,

$$\begin{aligned}
\mathcal{M}_\chi &= \frac{ic_\chi c_\psi}{2m_G^2\Lambda^2}\langle N(p_2)|\left(2\tilde{T}^\chi_{\mu\nu}\tilde{T}^{\psi,\mu\nu} - \frac{1}{6}T^\chi T^\psi\right)|N(p_1)\rangle \\
&= \frac{ic_\chi c_\psi}{2m_G^2\Lambda^2}\left\{\frac{1}{8}F_T\left[\frac{(P\cdot K)}{2m_\chi m_N}\left((K\cdot P)(\bar{u}_\chi(k_2)u_\chi(k_1))(\bar{u}_N(p_2)u_N(p_1))\right.\right.\right. \\
&\quad +(\bar{u}_\chi(k_2)u_\chi(k_1))(K_\nu\bar{u}_N(p_2)i\sigma^{\nu\lambda}q_\lambda u_N(p_1)) \\
&\quad -(P_\mu\bar{u}_\chi(k_2)i\sigma^{\mu\rho}q_\rho u_\chi(k_1))(\bar{u}_N(p_2)u_N(p_1)) \\
&\quad \left.\left.-(\bar{u}_\chi(k_2)i\sigma^{\mu\rho}q_\rho u_\chi(k_1))(\bar{u}_N(p_2)i\sigma_{\mu\lambda}q^\lambda u_N(p_1))\right)\right. \\
&\quad -4m_\chi m_N(\bar{u}_\chi(k_2)u_\chi(k_1))(\bar{u}_N(p_2)u_N(p_1)) \\
&\quad +\frac{1}{2m_\chi m_N}\left((K\cdot P)^2(\bar{u}_\chi(k_2)u_\chi(k_1))(\bar{u}_N(p_2)u_N(p_1))\right. \\
&\quad -(P_\mu\bar{u}_\chi(k_2)i\sigma^{\mu\rho}q_\rho u_\chi(k_1))(K_\nu\bar{u}_N(p_2)i\sigma^{\nu\lambda}q_\lambda u_N(p_1)) \\
&\quad +(K\cdot P)(\bar{u}_\chi(k_2)u_\chi(k_1))(K_\nu\bar{u}_N(p_2)i\sigma^{\nu\lambda}q_\lambda u_N(p_1)) \\
&\quad \left.\left.-(K\cdot P)(P_\mu\bar{u}_\chi(k_2)i\sigma^{\mu\rho}q_\rho u_\chi(k_1))(\bar{u}_N(p_2)u_N(p_1))\right)\right] \\
&\quad \left.-\frac{1}{6}m_\chi m_N F_S(\bar{u}_\chi(k_2)u_\chi(k_1))(\bar{u}_N(p_2)u_N(p_1))\right\}.
\end{aligned} \tag{4.30}$$

Therefore, there appear five effective interactions between fermion dark matter and nucleon due to the spin-2 mediator, each of which matches with non-relativistic operators [37] as in Table 4.3. Here, we note that the non-relativistic nucleon operators are given [37] by

$$\begin{aligned}
\mathcal{O}_1^{\rm NR} &= 1, \quad \mathcal{O}_2^{\rm NR} = (v^\perp)^2, \quad \mathcal{O}_3^{\rm NR} = i\vec{s}_N\cdot(\frac{\vec{q}}{m_N}\times\vec{v}^\perp), \\
\mathcal{O}_4^{\rm NR} &= \vec{s}_\chi\cdot\vec{s}_N, \quad \mathcal{O}_5^{\rm NR} = i\vec{s}_\chi\cdot(\frac{\vec{q}}{m_N}\times\vec{v}^\perp) \quad \mathcal{O}_6^{\rm NR} = (\vec{s}_\chi\cdot\frac{\vec{q}}{m_N})(\vec{s}_N\cdot\frac{\vec{q}}{m_N}).
\end{aligned} \tag{4.31}$$

Here, $\vec{s}_\chi, \vec{s}_N$ are the spins of dark matter and nucleon, respectively, and the momentum transfer $i\vec{q}$ and the relative velocity between dark matter and nucleon after scattering $\vec{v}^\perp$ are Galilean, Hermitian invariants [37]. There is a relation of these quantities as follows

$$\vec{v}^\perp = \vec{v} + \frac{\vec{q}}{2\mu_N} \tag{4.32}$$

where $\vec{v}$ is the initial relative velocity and μ_N is the reduced mass of the DM-nucleon system and it satisfies $\vec{v}^{\perp}\cdot\vec{q}=0$. We note that $\mathcal{O}^{\rm NR}_{1,2,3}$ give rise to only the spin-independent elastic scattering while $\mathcal{O}^{\rm NR}_{4,5,6}$ lead to the spin-dependent elastic scattering. All the appearing operators are T-even and P-even.

	$\mathcal{O}_i$	$\sum_k \mathcal{O}_k^{\rm NR}$
F	$(\bar{\chi}\chi)\left(\bar{N}N\right)$	$4m_\chi m_N\mathcal{O}_1^{NR}$
F	$(\bar{\chi}\chi)\left(K_\nu\bar{N}i\sigma^{\nu\lambda}q_\lambda N\right)$	$4m_\chi^2\vec{q}^2\mathcal{O}_1^{NR}-16m_\chi^2m_N^2\mathcal{O}_3^{NR}$
F	$(P_\mu\bar{\chi}i\sigma^{\mu\rho}q_\rho\chi)\left(\bar{N}N\right)$	$-4m_N^2\vec{q}^2\mathcal{O}_1^{NR}+16m_\chi m_N^3\mathcal{O}_5^{NR}$
F	$(\bar{\chi}i\sigma^{\mu\rho}q_\rho\chi)\left(\bar{N}i\sigma^{\nu\lambda}q_\lambda N\right)$	$16m_\chi m_N(\vec{q}^2\mathcal{O}_4^{NR}-m_N^2\mathcal{O}_6^{NR})$
F	$(P_\mu\bar{\chi}i\sigma^{\mu\rho}q_\rho\chi)\left(K_\nu\bar{N}i\sigma^{\nu\lambda}q_\lambda N\right)$	$-4m_\chi m_N(\vec{q}^2\mathcal{O}_1^{NR}-4m_N^2\mathcal{O}_3^{NR})$ $\times(\vec{q}^2\mathcal{O}_1^{NR}-4m_\chi m_N\mathcal{O}_5^{NR})$
S	$(S^*S)(\bar{N}N)$	$2m_N\mathcal{O}_1^{NR}$
S	$i(S^*\partial_\mu S-S\partial_\mu S^*)(\bar{N}\gamma^\mu N)$	$4m_Sm_N\mathcal{O}_1^{NR}$
V	$\bar{N}N$	$2m_Nf(\epsilon_1,\epsilon_2^*)\mathcal{O}_1^{\rm NR}$
V	$\epsilon^\alpha_{1,2}\bar{N}i\sigma_{\alpha\lambda}q^\lambda N$	$4im_N^2\left(\vec{s}_N\cdot(\vec{\epsilon}_{1,2}\times\frac{\vec{q}}{m_N})\right)$
V	$4im_N^2\left(\vec{s}_N\cdot(\vec{\epsilon}_{1,2}\times\frac{\vec{q}}{m_N})\right)$	$m_\chi\left(\vec{q}^2\mathcal{O}_1^{\rm NR}-4m_N^2\mathcal{O}_3^{\rm NR}\right)$

Table 4.3: Effective operators for fermion (F), scalar (S) and vector (V) dark matter.

As a result, from the scattering amplitude at the nucleon level given in equation (4.30), the effective interactions between fermion dark matter and nucleons are given by

$$\begin{aligned}\mathcal{L}_{\chi,\rm eff} &= \frac{c_\chi c_\psi}{2m_G^2\Lambda^2}\Bigg[\Bigg\{F_T\left(\frac{1}{2}(P\cdot K)^2+\frac{m_\chi}{2m_N}(P\cdot K)q^2+\frac{m_N}{2m_\chi}(P\cdot K)q^2-2m_\chi^2m_N^2+\frac{1}{4}q^2\right)\\ &\quad-\frac{2}{3}F_Sm_\chi^2m_N^2\Bigg\}\mathcal{O}_1^{\rm NR}-F_Tm_N\left(2m_\chi(P\cdot K)+m_Nq^2\right)\mathcal{O}_3^{\rm NR}-F_T(P\cdot K)q^2\mathcal{O}_4^{\rm NR}\\ &\quad-F_Tm_N\left(2m_N(P\cdot K)+m_\chi q^2\right)\mathcal{O}_5^{\rm NR}+F_Tm_N^2(P\cdot K)\mathcal{O}_6^{\rm NR}+4F_Tm_N^3m_\chi\mathcal{O}_3^{\rm NR}\mathcal{O}_5^{\rm NR}\Bigg].\end{aligned} \tag{4.33}$$

Then, using equation (4.28), the above effective Lagrangian becomes

$$\begin{aligned}\mathcal{L}_{\chi,\rm eff} &= \frac{c_\chi c_\psi}{2m_G^2\Lambda^2}\Bigg[\Bigg\{F_T\left(6m_\chi^2m_N^2+2(m_\chi^2+m_N^2)\vec{q}^2+\frac{\vec{q}^4}{4}\right)-\frac{2}{3}F_Sm_\chi^2m_N^2\Bigg\}\mathcal{O}_1^{\rm NR}\\ &\quad-F_Tm_N^2\left(8m_\chi^2+\vec{q}^2\right)\mathcal{O}_3^{\rm NR}-4m_\chi m_NF_T\,\vec{q}^2\mathcal{O}_4^{\rm NR}-F_Tm_Nm_\chi\left(8m_N^2+\vec{q}^2\right)\mathcal{O}_5^{\rm NR}\\ &\quad+4m_\chi m_N^3F_T\mathcal{O}_6^{\rm NR}+4F_Tm_N^3m_\chi\mathcal{O}_3^{\rm NR}\mathcal{O}_5^{\rm NR}\Bigg].\end{aligned} \tag{4.34}$$

Here, we note that a factor $\int\frac{d^3p}{(2\pi)^3\sqrt{2E}}\,a_N^{(\dagger)}$ per each nucleon state or $\int\frac{d^3p}{(2\pi)^3\sqrt{2E}}\,a_\chi^{(\dagger)}$ per

each dark matter state, with dimension E, are to be multiplied as overall factors such that the above effective Lagrangian for nucleons has a dimension 4.

For a zero momentum transfer with $\vec{q} = 0$, the above effective Lagrangian (4.33) is reduced to scalar operators $\mathcal{O}_1^{\rm NR}$ only, that are relevant for the usual computation of the total cross section. But, other operators also contribute to the differential cross section with respect to the momentum transfer or the recoil energy.

4.1.2 Scalar dark matter

The energy-momentum tensor for a scalar DM S is, in momentum space,

$$T^S_{\mu\nu} = -\Big(m_S^2\eta_{\mu\nu} + C_{\mu\nu,\alpha\beta}k_1^\alpha k_2^\beta\Big) \tag{4.35}$$

where

$$C_{\mu\nu,\alpha\beta} \equiv \eta_{\mu\alpha}\eta_{\nu\beta} + \eta_{\nu\alpha}\eta_{\mu\beta} - \eta_{\mu\nu}\eta_{\alpha\beta} \tag{4.36}$$

and the scalar DM is incoming into the vertex with momentum k_1 and is outgoing from the vertex with momentum k_2. Then, the trace part of the energy-momentum tensor is given by

$$T^S = -\Big(4m_S^2 - 2(k_1\cdot k_2)\Big), \tag{4.37}$$

and the traceless part is given by

$$\tilde{T}^S_{\mu\nu} = -\Big(k_{1\mu}k_{2\nu} + k_{2\mu}k_{1\nu} - \frac{1}{2}\eta_{\mu\nu}(k_1\cdot k_2)\Big). \tag{4.38}$$

We consider the elastic scattering between the DM scalar and the nucleon, $S(k_1) + N(p_1) \to S(k_2) + N(p_2)$, where the nucleon is incoming into the vertex with momentum p_1 and it is outgoing with momentum p_2. Doing as in the fermion case, from equation (4.38) and equation (4.18), the relevant effective interactions for the traceless parts are

$$\begin{aligned} 4\tilde{T}^S_{\mu\nu}\langle N(p_2)|\tilde{T}^{\psi,\mu\nu}|N(p_1)\rangle &= F_T\Big(2\bar{u}_N(p_2)(\not{k}_1 k_2\cdot(p_1+p_2) + \not{k}_2 k_1\cdot(p_1+p_2))u_N(p_1) \\ &\quad -2m_N(k_1\cdot k_2)(\bar{u}_N(p_2)u_N(p_1))\Big) \end{aligned} \tag{4.39}$$

Therefore, using $k_1\cdot(p_1+p_2) = k_2\cdot(p_1+p_2) = (s-u)/2$ and Gordon identity, we can rewrite the above result as

$$\begin{aligned} 4\tilde{T}^S_{\mu\nu}\langle N(p_2)|\tilde{T}^{\psi,\mu\nu}|N(p_1)\rangle &= F_T\Big[\frac{(P\cdot K)}{2m_N}\Big((P\cdot K)(\bar{u}_N(p_2)u_N(p_1)) + K_\nu\bar{u}_N(p_2)i\sigma^{\nu\lambda}q_\lambda u_N(p_1)\Big) \\ &\quad -2m_N(k_1\cdot k_2)(\bar{u}_N(p_2)u_N(p_1))\Big]. \end{aligned} \tag{4.40}$$

In a similar way, the effective interactions for the trace part is

$$4T^S\langle N(p_2)|T^\psi|N(p_1)\rangle = 8m_N F_S(2m_S^2 - k_1\cdot k_2)\,(\bar{u}_N(p_2)u_N(p_1)). \tag{4.41}$$

Consequently, from equations (4.40) and (4.41), we get that the scattering amplitude between scalar dark matter and nucleon is

$$\begin{aligned}\mathcal{M}_S &= \frac{ic_S c_\psi}{2m_G^2\Lambda^2}\,\langle N(p_2)|\left(2\tilde{T}^S_{\mu\nu}\tilde{T}^{\psi,\mu\nu} - \frac{1}{6}T^S T^\psi\right)|N(p_1)\rangle \\ &= \frac{ic_S c_\psi}{2m_G^2\Lambda^2}\left[F_T\left(\frac{(P\cdot K)}{4m_N}\left((P\cdot K)(\bar{u}_N(p_2)u_N(p_1)) + (K_\nu\bar{u}_N(p_2)i\sigma^{\nu\lambda}q_\lambda u_N(p_1))\right)\right.\right. \\ &\quad \left.\left. -m_N(k_1\cdot k_2)(\bar{u}_N(p_2)u_N(p_1))\right) - \frac{1}{3}m_N F_S(2m_S^2 - k_1\cdot k_2)\,(\bar{u}_N(p_2)u_N(p_1))\right]\end{aligned} \tag{4.42}$$

Here, we note that using the Gordon identity, the tensor operator $\bar{N}i\sigma^{\nu\lambda}q_\lambda N$ can be written as the sum of vector and scalar operators.

Therefore, there appear two effective interactions between scalar dark matter and nucleon due to the spin-2 mediator, each of which matches to the non-relativistic nucleon operator [83] as shown in Table 4.3. We can see that only the scalar operator at the non-relativistic level appears for scalar dark matter. Now from equation (4.42), we obtain the effective Lagrangian for scalar dark matter as follows

$$\mathcal{L}_{S,\text{eff}} = \frac{c_S c_\psi}{2m_G^2\Lambda^2}\left[2F_T\left(m_S m_N(P\cdot K) - m_N^2(k_1\cdot k_2)\right) - \frac{2}{3}F_S m_N^2(2m_S^2 - k_1\cdot k_2)\right]\mathcal{O}_1^{\text{NR}} \tag{4.43}$$

Using equation (4.28) and $q^2 \simeq 2\vec{k_2}\cdot\vec{k_1}$, the above effective Lagrangian becomes

$$\mathcal{L}_{S,\text{eff}} = \frac{c_S c_\psi}{2m_G^2\Lambda^2}\left[2F_T m_N^2\left(4m_S^2 - \frac{\vec{q}^2}{2}\right) - \frac{2}{3}F_S m_N^2(2m_S^2 - \frac{\vec{q}^2}{2})\right]\mathcal{O}_1^{\text{NR}}. \tag{4.44}$$

For a zero momentum transfer, the above effective Lagrangian (4.43) is reduced to scalar operators $\mathcal{O}_1^{\text{NR}}$ only.

4.2 Differential scattering event rates with spin-2 mediator

In this section, we discuss the differential event rates for the spin-independent scattering between dark matter and nucleus in our model, for mock and current experiments of dark matter direct detection.

To compute the differential scattering event rates in our model, we take the model parameters that are consistent with the limits from DM direct detection experiments and use the package called DMFormFactor [37, 91] to perform this computation.

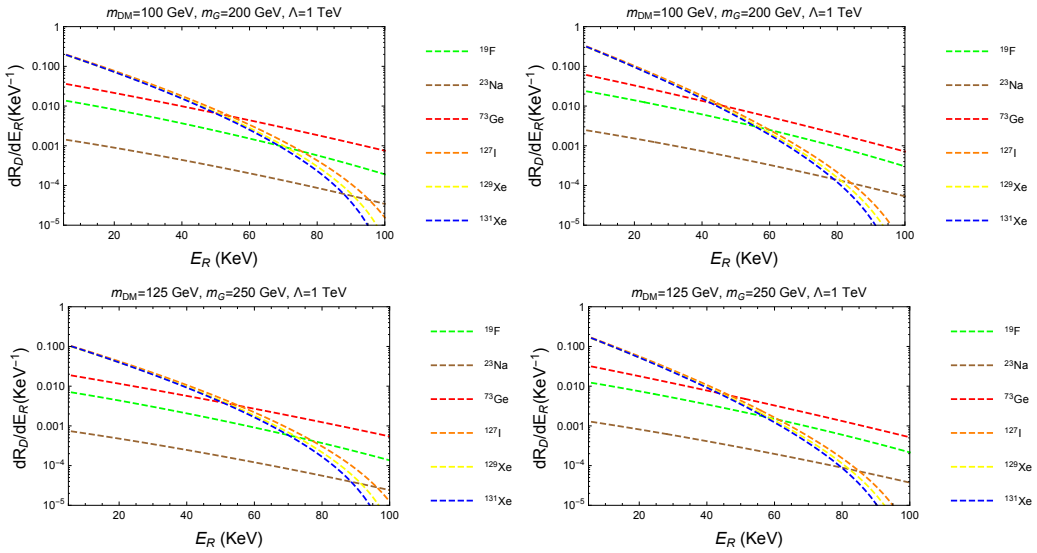

Figure 4.2: Differential event rates for fermionic dark matter (left) and scalar dark matter (right) for different experiments in Table 4.4 for $\Lambda = 1$ TeV and $c_\chi = c_\psi = 1$.

Nucleus	Z	A	Exposure (Kg-day)
F	9	19	200000
Na	11	23	14000
Ge	32	73	36500
I	53	127	78000
Xe	54	129	73000
Xe	54	131	73000

Table 4.4: Mock experiments considered for the computation of differential scattering event rates in this model.

The input parameters for the package of DMFormFactor [37,91] are the spin and mass of DM, the information about the Galactic Halo (such as the escape velocity and the local DM density), our model parameters such as the couplings and mass of the graviton and the scale Λ, and finally the information about the detector we are considering. In our case, we use the parameters for different mock experiments with some of the most relevant isotopes as shown in Table 4.4. Using the information in Table 4.4, the Lagrangians for the interactions in (4.34) and (4.44) and taking a zero momentum transfer $q \to 0$ approximation, we obtain the results for the differential event rates as a function of the recoil energy (E_R) in units of keV as in Figs. (4.2) and (4.3), for the cases with fermionic and scalar dark matter for $\Lambda = 1$ TeV and 3 TeV, respectively. For the fermionic case, the

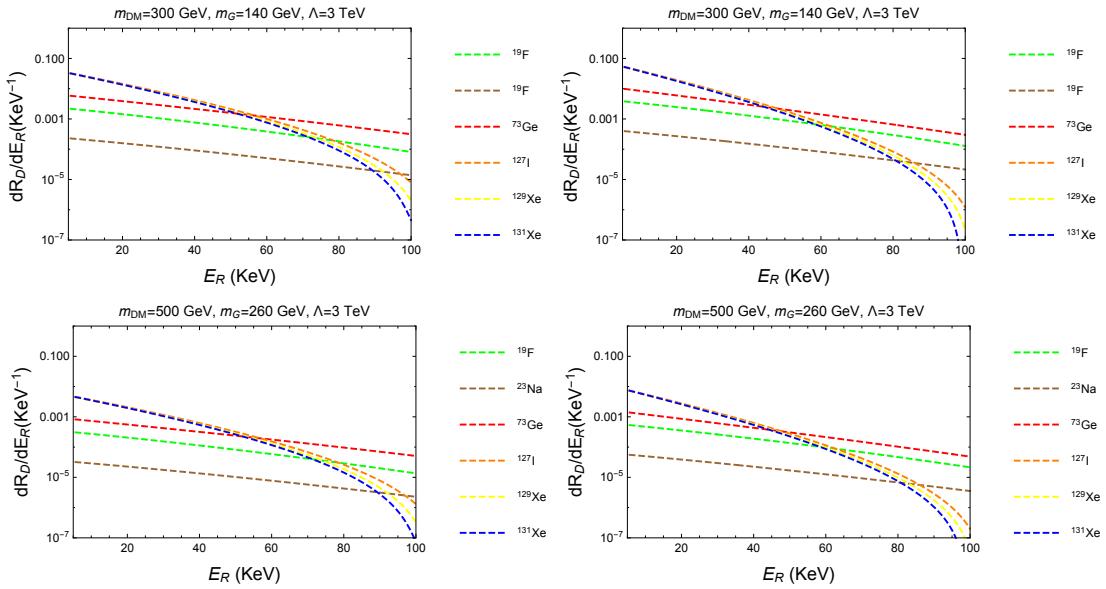

Figure 4.3: The same as in Fig. 4.2, but with different masses for DM and spin–2 mediators and $\Lambda = 3$ TeV.

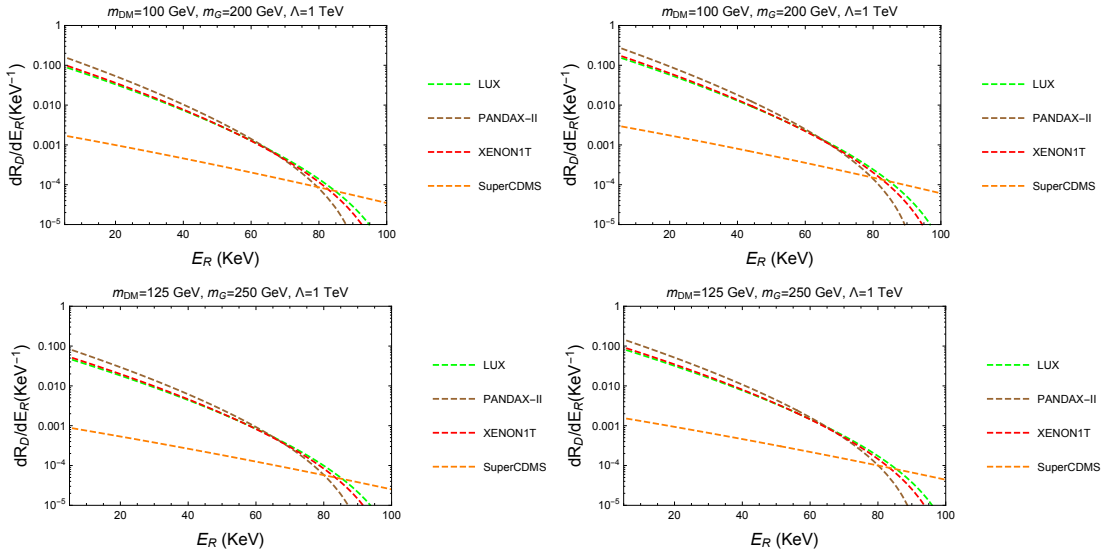

Figure 4.4: Differential event rates for fermion DM (left) and scalar DM (right) for current experiments for $\Lambda = 1$ TeV and $c_\chi = c_\psi = 1$.

last operator in the Lagrangian $\mathcal{O}_3^{\rm NR}\mathcal{O}_5^{\rm NR}$ is a new type of interaction term that is allowed when the mediator is a spin 2 particle. But, the $\mathcal{O}_3^{\rm NR}\mathcal{O}_5^{\rm NR}$ term is velocity-suppressed so it is not included in our study. Therefore, the differential event rates for fermion and scalar dark matter are similar when the DM mass and the mass and coupling of the spin-2 mediator are the same but later it will be shown that the annihilation cross sections of dark matter crucially depend on the spin of dark matter.

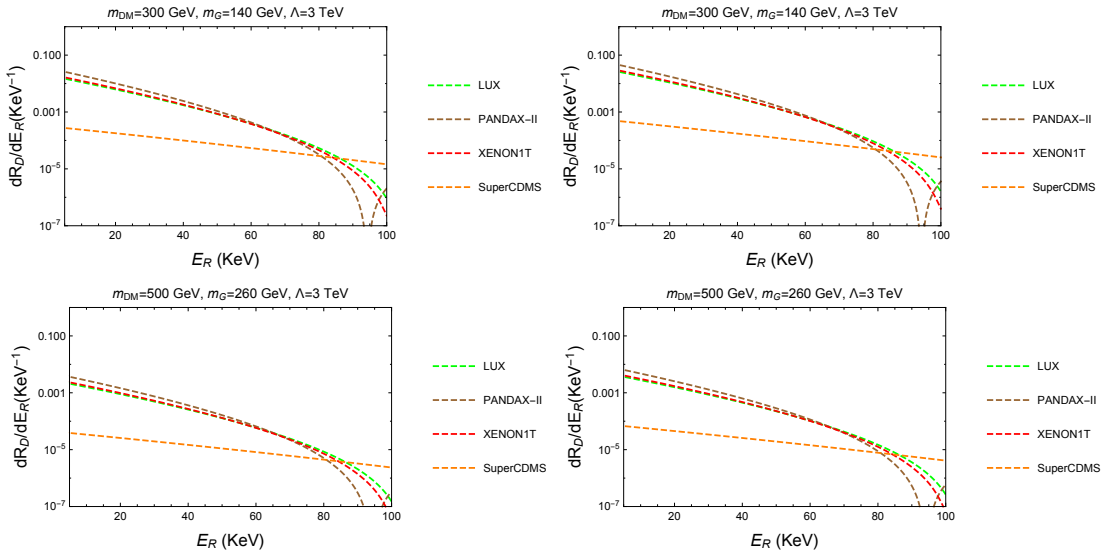

Figure 4.5: The same as in Fig. 4.4 but considering different masses for DM and spin-2 mediators and a value of $\Lambda = 3$ TeV.

Experiment (Nucleus)	Z	A	Exposure (Kg-day)
LUX (Xe)	54	129	33500
XENON1T (Xe)	54	131	36500
PandaX-II (Xe)	54	136	54000
SuperCDMS (Ge)	32	73	1690
CDMSlite (Ge)	32	73	70
XENON10 (Xe)	54	131	15

Table 4.5: Detector information for the current experiments considering in this study for the computation of differential scattering event rates in this model.

Also, we obtained similar plots, considering the detectors used in current DM experiments as XENON1T [92], PandaX-II [22], SuperCDMS [25], LUX [93], CDMSlite [26], and XENON10 [94], with the detector parameters shown in Table 4.5. Some results for differential event rates with WIMP dark matter are shown in Figs. 4.4 and 4.5, for values of $\Lambda = 1$ TeV and 3 TeV, respectively, with the parameters that are consistent with other limits on the parameters space that came from relic density condition, ATLAS dijet and direct detection bounds that are discussed in the next section.

4.3 Bounds from relic density and direct detection

In this section we consider the annihilation cross sections for the different types of dark matter in order to determine the relic density and how this computation put conditions over the parameter space of our model. Then, we discuss a bit more the direct detection limits on the total spin-independent elastic scattering cross section and the dijet bounds on the spin-2 mediator from the LHC.

4.3.1 Fermion dark matter

The annihilation cross section for $\chi\bar{\chi} \to \psi\bar{\psi}$ is given [5, 42, 80] by

$$(\sigma v)_{\chi\bar{\chi}\to\psi\bar{\psi}} = v^2 \cdot \frac{N_c c_\chi^2 c_\psi^2}{72\pi\Lambda^4} \frac{m_\chi^6}{(4m_\chi^2 - m_G^2)^2 + \Gamma_G^2 m_G^2} \left(1 - \frac{m_\psi^2}{m_\chi^2}\right)^{\frac{3}{2}} \left(3 + \frac{2m_\psi^2}{m_\chi^2}\right). \quad (4.45)$$

Thus, the annihilation of fermion dark matter into quarks becomes p-wave suppressed. When $m_\chi > m_G$, there is an extra contribution to the annihilation cross section, due to the t-channel for both models [5, 42, 80], as follows,

$$(\sigma v)_{\chi\bar{\chi}\to GG} = \frac{c_\chi^4 m_\chi^2}{16\pi\Lambda^4} \frac{(1 - r_\chi)^{\frac{7}{2}}}{r_\chi^4 (2 - r_\chi)^2} \quad (4.46)$$

with $r_\chi = \left(\frac{m_G}{m_\chi}\right)^2$. Then, the t-channel annihilation is s-wave, so it becomes dominant in determining the relic density for heavy fermion dark matter.

4.3.2 Scalar dark matter

The annihilation cross section for $SS \to \psi\bar{\psi}$ is given [5, 42, 80] by

$$(\sigma v)_{SS\to\psi\bar{\psi}} = v^4 \cdot \frac{N_c c_S^2 c_\psi^2}{360\pi\Lambda^4} \frac{m_S^6}{(m_G^2 - 4m_S^2)^2 + \Gamma_G^2 m_G^2} \left(1 - \frac{m_\psi^2}{m_S^2}\right)^{\frac{3}{2}} \left(3 + \frac{2m_\psi^2}{m_S^2}\right). \quad (4.47)$$

Thus, the annihilation of scalar dark matter into quarks becomes d-wave suppressed.

When $m_S > m_G$, there is an extra contribution to the annihilation cross section, due to the t-channel for both models [5, 42, 80], as follows,

$$(\sigma v)_{SS\to GG} = \frac{4c_S^4 m_S^2}{9\pi\Lambda^4} \frac{(1 - r_S)^{\frac{9}{2}}}{r_S^4 (2 - r_S)^2} \quad (4.48)$$

with $r_S = \left(\frac{m_G}{m_S}\right)^2$.

4.3.3 Vector dark matter

The annihilation cross section for $XX \to \psi\bar{\psi}$ is given [5, 42, 80] by

$$(\sigma v)_{XX\to\psi\bar{\psi}} = \frac{4N_c c_X^2 c_\psi^2}{27\pi\Lambda^4}\frac{m_X^6}{(4m_X^2-m_G^2)^2+\Gamma_G^2 m_G^2}\left(3+\frac{2m_\psi^2}{m_X^2}\right)\left(1-\frac{m_\psi^2}{m_X^2}\right)^{\frac{3}{2}} \quad (4.49)$$

Thus, the annihilation of vector dark matter into quarks becomes s-wave suppressed. In this case, smaller spin-2 mediator couplings to the SM quarks or vector dark matter can be consistent with the correct relic density, as compared to the other cases. But, indirect detection signals from the annihilation of vector dark matter are promising [42].

As $m_X > m_G$, there is an extra contribution to the annihilation cross section, due to the t-channel in both models [5, 42, 80], as follows,

$$\begin{aligned}(\sigma v)_{XX\to GG} &= \frac{c_X^4 m_X^2}{324\pi\Lambda^4}\frac{\sqrt{1-r_X}}{r_X^4(2-r_X)^2}\Big(176+192r_X+1404r_X^2-3108r_X^3 \\ &\quad +1105r_X^4+362r_X^5+34r_X^6\Big) \end{aligned} \quad (4.50)$$

with $r_X = \left(\frac{m_G}{m_X}\right)^2$.

4.3.4 Bounds on WIMP dark matter

Taking a zero momentum transfer for the DM-nucleon scattering, we use the nucleon matrix elements for twist-2 operators given in equation (4.17) and simply obtain the total cross section for spin-independent elastic scattering between dark matter and nucleus as

$$\sigma^{SI}_{\mathrm{DM}-A} = \frac{\mu_A^2}{\pi}\left(Zf_p^{\mathrm{DM}}+(A-Z)f_n^{\mathrm{DM}}\right)^2 \quad (4.51)$$

where $\mu_A = m_\chi m_A/(m_\chi+m_A)$ is the reduced mass of the DM-nucleus system and m_A is the target nucleus mass, Z is the number of protons, A is the atomic number and the nucleon form factors are given by the same formula for all the spins of dark matter as

$$f_p^{\mathrm{DM}} = \frac{c_{\mathrm{DM}} m_N m_{\mathrm{DM}}}{4m_G^2\Lambda^2}\left(\sum_{\psi=u,d,s,c,b} 3c_\psi(\psi(2)+\bar{\psi}(2)) + \sum_{\psi=u,d,s}\frac{1}{3}c_\psi f_{T\psi}^p\right), \quad (4.52)$$

$$f_n^{\mathrm{DM}} = \frac{c_{\mathrm{DM}} m_N m_{\mathrm{DM}}}{4m_G^2\Lambda^2}\left(\sum_{\psi=u,d,s,c,b} 3c_\psi(\psi(2)+\bar{\psi}(2)) + \sum_{\psi=u,d,s}\frac{1}{3}c_\psi f_{T\psi}^n\right) \quad (4.53)$$

where $\mathrm{DM} = \chi, S, X$ for fermion, scalar and vector dark matter, respectively. The results are the same as those for the general effective interactions with zero momentum transfer in equation (4.34), (4.43) and (4.44).

The above DM-nucleus scattering cross section is related to the normalized-to-proton scattering cross section $\sigma^{SI}_{\mathrm{DM}-p}$, that is usually presented for experimental limits by

$$\sigma^{SI}_{\mathrm{DM}-p} = (\mu_N/\mu_A)^2\sigma^{\mathrm{SI}}_{\mathrm{DM}-A}/A^2 \quad (4.54)$$

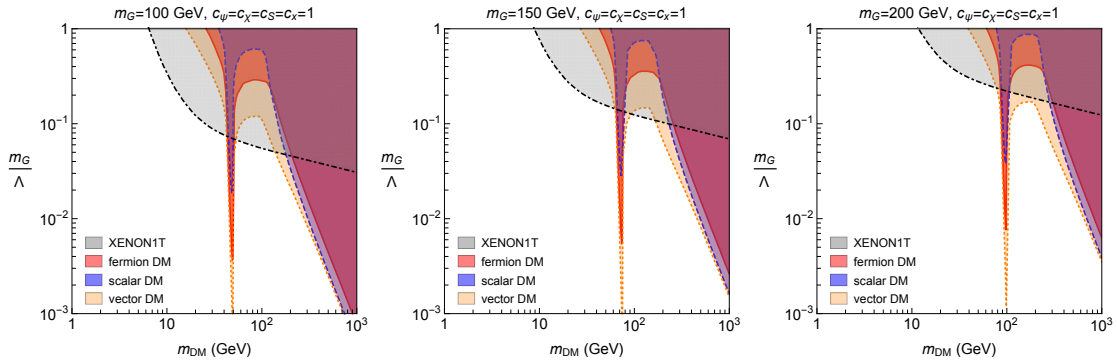

Figure 4.6: Parameter space of fermion and scalar dark matter in $m_{\rm DM}$ vs m_G/Λ. The gray regions are excluded by XENON1T. We took $c_\chi = c_S = c_{u,d,s,c,b,t} = 1$ and $m_G = 100, 150, 200\,\text{GeV}$ on left, middle and right, respectively.

with $\mu_N = m_{\rm DM} m_N/(m_{\rm DM} + m_N)$.

In Fig. 4.6, we depict in the parameter space for $m_{\rm DM}$ vs m_G/Λ the region where the DM relic density overcloses the Universe in red, blue and orange for fermion, scalar and vector dark matter, respectively. The regions in gray are ruled out by the direct detection experiment in XENON1T [92]. We have taken $m_G = 100, 150, 200\,\text{GeV}$ from left to right plots and the couplings of DM and quarks to the spin-2 mediator are the same as $c_\chi = c_S = c_{u,d,s,c,b,t} = 1$ in all the plots. As a result, we find that the non-resonance regions saturating the relic density, away from the resonance with $m_G \sim 2m_{\rm DM}$, are tightly constrained by XENON1T bounds. The non-resonance regions below $m_{\rm DM} = 200 - 300\,\text{GeV}$ have been already excluded, but the non-resonance regions with larger DM masses and the resonance region can be probed by updated XENON1T and future direct detection experiments.

In Fig. 4.7, we impose in the parameter space for $m_{\rm DM}$ vs m_G the same conditions from the relic density and the limits from XENON1T. The relic density is saturated by the DM annihilation into quarks along the red, blue and orange lines, for fermion, scalar and vector dark matter, respectively. The regions in gray are ruled out by the direct detection experiment in XENON1T [92]. We also overlaid in cyan regions the bounds from dijet resonance searches with mono-photon at the LHC [95]. In the case with $m_G > 2m_{\rm DM}$, for which the spin-2 mediator decays invisibly into a pair of dark matter, the ATLAS dijet limit on Λ scales by $\sqrt{\text{BR}(G \to q\bar{q})} = \sqrt{\frac{15}{19}}\left(\sqrt{\frac{15}{16}}\right)$ with $q = u, d, s, c, b$ for $m_G > 2m_t (m_G < 2m_t)$, which leads only to a very mild change in the cyan region in Fig. 4.7. We have taken $\Lambda = 1, 3, 5\,\text{TeV}$ from left to right plots and the same couplings of DM and quarks to the spin-2 mediator as $c_\chi = c_S = c_{u,d,s,c,b,t} = 1$ in all the plots. In the case with $\Lambda = 1\,\text{TeV}$, the WIMP parameter space, in particular, the non-resonance region,

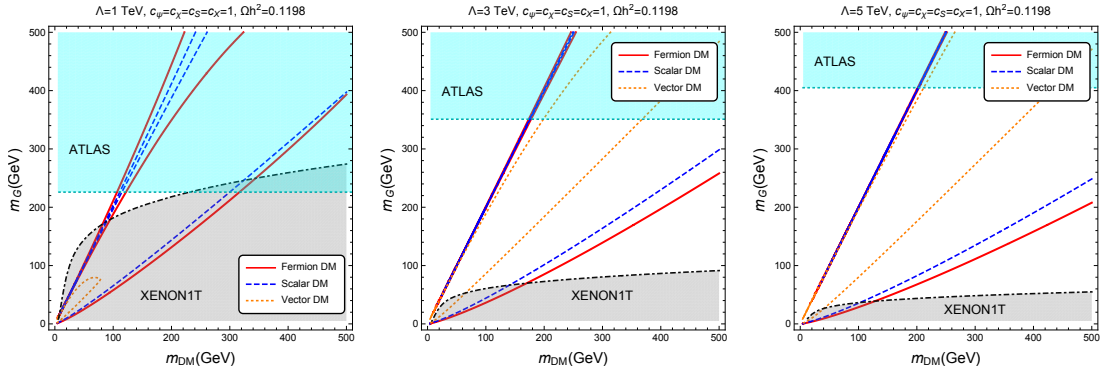

Figure 4.7: Parameter space of fermion and scalar dark matter in $m_{\rm DM}$ vs m_G. The gray and cyan regions are excluded by XENON1T and ATLAS dijet searches, respectively. The cyan regions was computed using MadGraph and the RS model. We took $\Lambda = 1, 3, 5\,\text{TeV}$ on left, middle and right, respectively. The other parameters are the same as in Fig. 4.6.

is tightly constrained by both XENON1T and dijet bounds. But, for larger values of $\Lambda = 3, 5\,\text{TeV}$, a wide parameter space opens up and can be tested by updated XENON1T and future experiments.

4.3.5 Bounds on light dark matter

Some results for the corresponding differential event rates with light fermion or scalar dark matter below 10 GeV are shown for CDMSlite and XENON10 experiments in Figs. 4.8 and 4.9. Here, we have chosen the parameters that are consistent with direct detection bounds, in particular, from XENON10 and cryogenic direct detection experiments such as CDMSlite and CRESST.

In Fig. 4.10, we considered the case with light dark matter of mass below 10 GeV. In this case, cryogenic direct detection experiments [96] such as CDMSlite [26] and CRESST [35] with low thresholds for recoil energy are relevant for $m_{\rm DM} = 1.45 - 9\,\text{GeV}$ and $0.71 - 9\,\text{GeV}$, respectively, and the CDMSlite experiment rules out the parameter space in green region too. We note that the bounds from CRESST or XENON10 are less stringent that the one from CDMSlite, so we don't show them in Fig. 4.10. We have taken $\Lambda = 1, 3, 5\,\text{TeV}$ from left to right plots and the couplings of DM and quarks to the spin-2 mediator are the same as $c_\chi = c_S = c_{u,d,s,c,b,t} = 1$ in all the plots. As a consequence, for a low $\Lambda = 1\,\text{TeV}$, the region where dark matter annihilation into a pair of spin-2 mediators explains the correct relic density is almost excluded by direct detection, except for $m_{\rm DM} \lesssim 2\,\text{GeV}$. The resonance region with $m_G \sim 2m_{\rm DM}$ survives the direct detection bounds. On the other

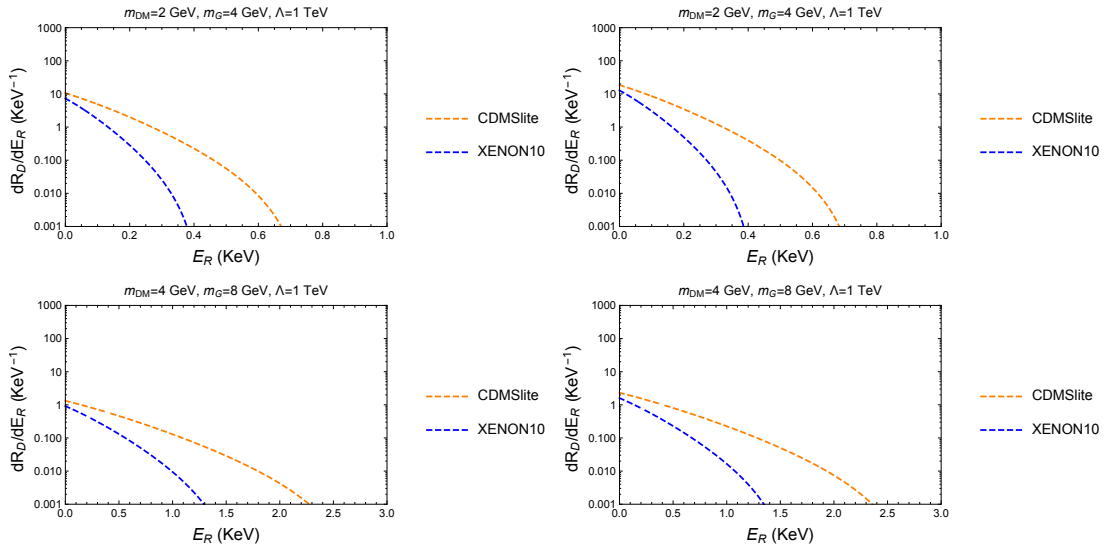

Figure 4.8: Differential event rates for light fermion (left) or scalar (right) dark matter for current experiments for $\Lambda = 1$ TeV and $c_\chi = c_\psi = 1$.

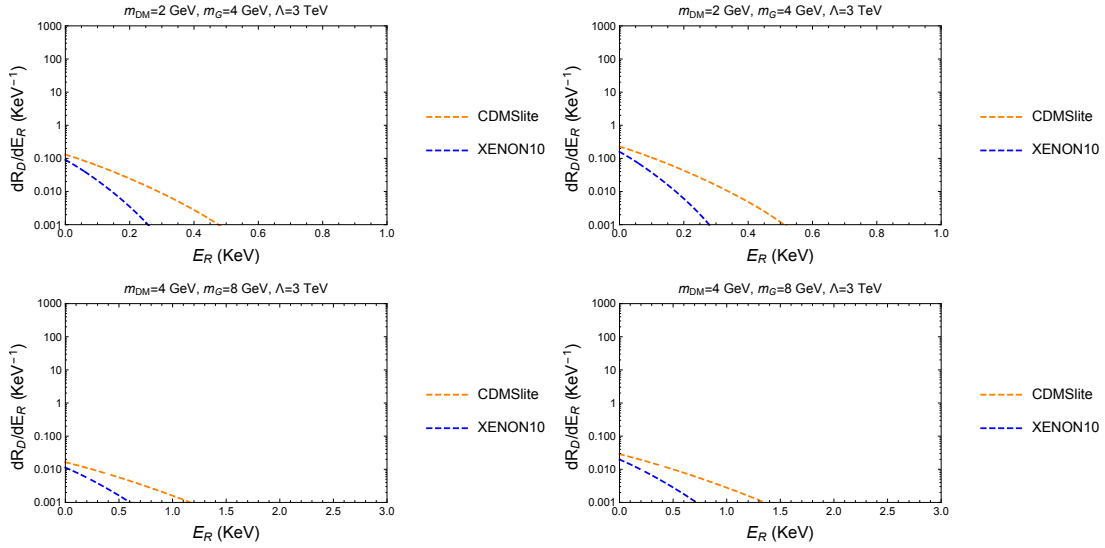

Figure 4.9: The same as in Fig. 4.8, but for $\Lambda = 3$ TeV.

hand, for larger values of $\Lambda = 3, 5$ TeV, the more non-resonance region below $m_{\rm DM} \simeq 6$ GeV survives.

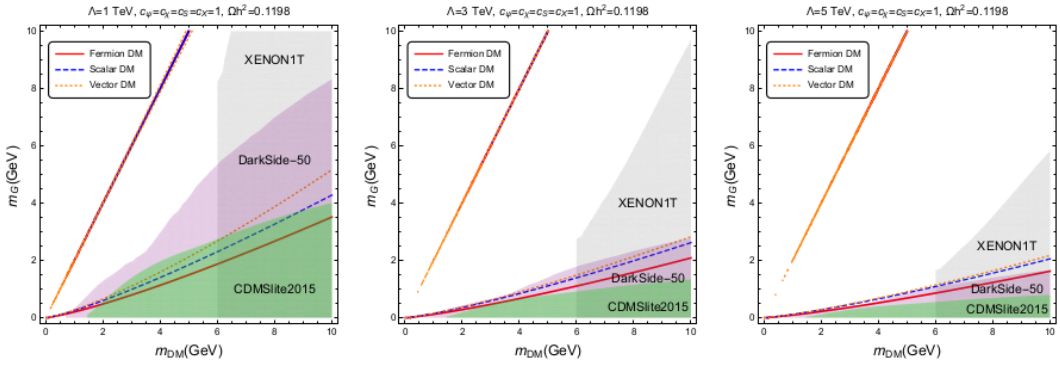

Figure 4.10: Parameter space of light dark matter below 10 GeV. The gray, green and purple regions are excluded by XENON1T, CDMSlite and DarkSide-50, respectively. We took $\Lambda = 1, 3, 5$ TeV on left, middle and right, respectively. The other parameters are the same as in Fig. 4.6.

Chapter 5

Conclusions

In this chapter, there are some remarks about the conclusion and results obtained in this work [6] and also a description of the future work that can be done exploring this model.

5.1 Conclusions

Direct detection limits on the interaction of DM-DM cross section are getting more restrictive with time and getting closer to the neutrino floor, as no signals of this interaction has been observed. This result may seen a bit dark in our search for answers about the origin and nature of DM but it still helps us to check the viability of the models proposed as solutions of the mentioned problem.

After all the computation presented in the previous chapter using the EFT techniques and the tools and packages that helps us performing the direct detection rates more easily, we obtained the expansion of the corresponding DM-SM interactions from the GMDM model that are important for the computation of direct detection limits. We passed using gravitational form factors from the quark world to the nucleon interaction.

From this expansion and then doing the corresponding matching of each term with the non-relativistic operators for nucleons, we found that this operators have specific correlations, depending on the spin of dark matter. We have to note 2 things: that in the fermion case a new term appeared in the expansion that needs to be explore in more detail and that in the vector case, we found also new terms that could not been match with the NR operators known for vector particles and these terms need to be study more deeply.

All this work, done for each type of DM, allow us to compute and show the differential event rates for spin-independent DM-nucleon scattering at current direct detection exper-

iments and for some mock experiments that explore the use of different material in the construction of the corresponding detector.

We were able to impose bounds on the parameter space (for the mass and couplings of the spin-2 mediator) of the GMDM model coming from the limits on the DM-SM cross section obtained from the latest and more restrictive direct detection experiment XENON1T and also we used the relic density condition as well as the LHC dijet searches to set extra constrains on this parameter space. We did this for the heavy (mass order of WIMPs) and for light DM cases.

We can extend this work doing a more detail exploration of the interaction terms in the mentioned cases (fermion and vector DM) as the way how to deal with them to further computations (for example, if it is possible to extend the current tools to include them) and also we need to include the interaction with the gluons, as in the first place we just worked with the quark terms, that will add some extra information and then we can explore a bit more the rates for the current or future experiments to see if any of them can be able to see a signal produced by this process.

Bibliography

[1] R. Adam et al. Planck 2015 results. *Astronomy & Astrophysics*, 594:A1, oct 2016. 1, 3

[2] E W Kolb and M S Turner. *The Early Universe*. Frontiers in Physics. Addison-Wesley, 1990. 1, 3, 7, 8, 11, 12, 17

[3] Gianfranco Bertone, Dan Hooper, and Joseph Silk. Particle dark matter: evidence, candidates and constraints. *Physics Reports*, 405(5-6):279–390, jan 2005. 1, 6, 8

[4] Mariangela Lisanti. Lectures on Dark Matter Physics. In *New Frontiers in Fields and Strings*, pages 399–446. WORLD SCIENTIFIC, jan 2017. 1

[5] Hyun Min Lee, Myeonghun Park, and Verónica Sanz. Gravity-mediated (or composite) dark matter. *The European Physical Journal C*, 74(2):2715, feb 2014. ix, 2, 19, 22, 25, 26, 39, 40

[6] A Carrillo-Monteverde, Yoo-jin Kang, Hyun Min Lee, Myeonghun Park, and Veronica Sanz. Dark matter direct detection from new interactions in models with spin-two mediators. *Journal of High Energy Physics*, 2018(6):37, jun 2018. 2, 45

[7] F. Zwicky. On the Masses of Nebulae and of Clusters of Nebulae. *Astrophys. J.*, 86:217–246, 1937. 3

[8] E Papantonopoulos. *The Physics Of The Early Universe*. Lecture Notes in Physics. Springer, 2005. 4

[9] A V Zasov, A S Saburova, A V Khoperskov, and S A Khoperskov. Dark matter in galaxies. *Physics-Uspekhi*, 60(1):3–39, jan 2017. ix, 4

[10] Volker Springel et al. Simulating the joint evolution of quasars, galaxies and their large-scale distribution. *Nature*, 435:629–636, 2005. ix, 5

[11] Marco Taoso, Gianfranco Bertone, and Antonio Masiero. Dark matter candidates: a ten-point test. *Journal of Cosmology and Astroparticle Physics*, 2008(03):022, mar 2008. 7

[12] J Beringer et al. Review of Particle Physics. *Physical Review D*, 86(1):010001, jul 2012. 7, 16

[13] Gerard Jungman, Marc Kamionkowski, and Kim Griest. Supersymmetric dark matter. *Physics Reports*, 267(5-6):195–373, mar 1996. 11

[14] Laura Baudis. Dark matter searches. *Annalen Phys.*, 528:74–83, 2016. ix, 11

[15] Jennifer M. Gaskins. A review of indirect searches for particle dark matter. *Contemp. Phys.*, 57(4):496–525, 2016. 14

[16] Carlos A. Argelles, Ali Kheirandish, Jeffrey Lazar, and Qinrui Liu. Search for Dark Matter Annihilation to Neutrinos from the Sun. *PoS*, ICRC2019:527, 2020. 15

[17] Jianglai Liu, Xun Chen, and Xiangdong Ji. Current status of direct dark matter detection experiments. *Nature Physics*, 13(3):212–216, mar 2017. 15

[18] Teresa Marrodn Undagoitia and Ludwig Rauch. Dark matter direct-detection experiments. *J. Phys. G*, 43(1):013001, 2016. 15

[19] C. Amole et al. Dark Matter Search Results from the Complete Exposure of the PICO-60 C_3F_8 Bubble Chamber. *Phys. Rev. D*, 100(2):022001, 2019. 16

[20] Marc Schumann. Direct Detection of WIMP Dark Matter: Concepts and Status. *J. Phys. G*, 46(10):103003, 2019. 16

[21] E. Aprile et al. Dark Matter Search Results from a One Ton-Year Exposure of XENON1T. *Physical Review Letters*, 121(11):1–8, 2018. 16

[22] Xiangyi Cui et al. Dark Matter Results from 54-Ton-Day Exposure of PandaX-II Experiment. *Physical Review Letters*, 119(18):181302, oct 2017. 16, 38

[23] B. J. Mount et al. LUX-ZEPLIN (LZ) Technical Design Report. mar 2017. 16

[24] P. Agnes et al. DarkSide-50 532-day dark matter search with low-radioactivity argon. *Physical Review D*, 98(10):102006, nov 2018. 16

[25] R. Agnese et al. Results from the Super Cryogenic Dark Matter Search Experiment at Soudan. *Physical Review Letters*, 120(6):061802, feb 2018. 16, 38

[26] R. Agnese et al. New Results from the Search for Low-Mass Weakly Interacting Massive Particles with the CDMS Low Ionization Threshold Experiment. *Physical Review Letters*, 116(7):071301, feb 2016. 16, 38, 42

[27] Ke-Jun Kang et al. CDEX-1 1 kg point-contact germanium detector for low mass dark matter searches. *Chinese Physics C*, 37(12):126002, dec 2013. 16

[28] Mariangela Settimo. The DAMIC experiment at SNOLAB. may 2018. 16

[29] E. Behnke et al. Final results of the PICASSO dark matter search experiment. *Astroparticle Physics*, 90:85–92, apr 2017. 16

[30] C. Amole et al. Dark Matter Search Results from the PICO-60 C$_3$F$_8$ Bubble Chamber. *Physical Review Letters*, 118(25):251301, jun 2017. 16

[31] E. Behnke et al. Direct Measurement of the Bubble Nucleation Energy Threshold in a CF3I Bubble Chamber. *Physical Review D*, 88(2):021101, jul 2013. 16

[32] R. Bernabei et al. DAMA/LIBRA Results and Perspectives. *EPJ Web of Conferences*, 182:02027, aug 2018. 16

[33] Hyun Su Lee. The status of KIMS-NaI experiment. *Nuclear and Particle Physics Proceedings*, 273-275:295–301, apr 2016. 16

[34] W. G. Thompson and for the COSINE-100 Collaboration. Current status and projected sensitivity of COSINE-100. nov 2017. 16

[35] G. Angloher et al. Results on light dark matter particles with a low-threshold CRESST-II detector. *The European Physical Journal C*, 76(1):25, jan 2016. 16, 42

[36] Marc Schumann. Direct Detection of WIMP Dark Matter: Concepts and Status. *J. Phys. G*, 46(10):103003, 2019. ix, 17

[37] Nikhil Anand, A Liam Fitzpatrick, and W C Haxton. Model-independent Analyses of Dark-Matter Particle Interactions. *Physics Procedia*, 61:97–106, 2015. 17, 18, 32, 35, 36

[38] Teresa Marrodán Undagoitia and Ludwig Rauch. Dark matter direct-detection experiments. *Journal of Physics G: Nuclear and Particle Physics*, 43(1):13001, jan 2016. 18

[39] Juan Herrero-Garcia, Thomas Schwetz, and Jure Zupan. On the annual modulation signal in dark matter direct detection. *JCAP*, 03:005, 2012. 18

[40] R. Bernabei et al. First results from DAMA/LIBRA and the combined results with DAMA/NaI. *Eur. Phys. J. C*, 56:333–355, 2008. 18

[41] C.E. Aalseth et al. Search for an Annual Modulation in a P-type Point Contact Germanium Dark Matter Detector. *Phys. Rev. Lett.*, 107:141301, 2011. 18

[42] Hyun Min Lee, Myeonghun Park, and Verónica Sanz. Gravity-mediated (or composite) Dark Matter confronts astrophysical data. *Journal of High Energy Physics*, 2014(5):63, may 2014. 19, 25, 39, 40

[43] Th. Kaluza. Zum Unittsproblem der Physik. *Sitzungsber. Preuss. Akad. Wiss. Berlin (Math. Phys.)*, 1921:966–972, 1921. [Int. J. Mod. Phys.D27,no.14,1870001(2018)]. 19

[44] Oskar Klein. Quantum Theory and Five-Dimensional Theory of Relativity. (In German and English). *Z. Phys.*, 37:895–906, 1926. [Surveys High Energ. Phys.5,241(1986)]. 19

[45] EDUARDO PONTN. *Four Lectures on TeV Scale Extra Dimensions*, pages 283–374. 19

[46] Nima ArkaniHamed, Savas Dimopoulos, and Gia Dvali. The hierarchy problem and new dimensions at a millimeter. *Physics Letters B*, 429(3):263 – 272, 1998. 20

[47] Ignatios Antoniadis, Nima Arkani-Hamed, Savas Dimopoulos, and Gia Dvali. New dimensions at a millimeter to a fermi and superstrings at a tev. *Physics Letters B*, 436(3):257 – 263, 1998. 20

[48] Gary Shiu and S.-H. Henry Tye. Tev scale superstring and extra dimensions. *Phys. Rev. D*, 58:106007, Oct 1998. 20

[49] Keith R. Dienes, Emilian Dudas, and Tony Gherghetta. Grand unification at intermediate mass scales through extra dimensions. *Nuclear Physics B*, 537(1):47 – 108, 1999. 20

[50] Lisa Randall and Raman Sundrum. Large Mass Hierarchy from a Small Extra Dimension. *Physical Review Letters*, 83(17):3370–3373, oct 1999. 20

[51] Merab Gogberashvili. FOUR DIMENSIONALITY IN NON-COMPACT KALUZA-KLEIN MODEL. *Modern Physics Letters A*, 14(29):2025–2031, sep 1999. 20

[52] Walter D. Goldberger and Mark B. Wise. Modulus stabilization with bulk fields. *Phys. Rev. Lett.*, 83:4922–4925, Dec 1999. 20

[53] Kingman Cheung. Phenomenology of the radion in the randall-sundrum scenario. *Phys. Rev. D*, 63:056007, Feb 2001. 21

[54] John Ellis and Keith A. Olive. Supersymmetric Dark Matter Candidates. pages 142–163, 1 2010. 21

[55] John R. Ellis et al. Supersymmetric Relics from the Big Bang. *Nucl. Phys. B*, 238:453–476, 1984. 21

[56] H. Goldberg. Constraint on the photino mass from cosmology. *Phys. Rev. Lett.*, 50:1419–1422, May 1983. 21

[57] I. Antoniadis. A possible new dimension at a few tev. *Physics Letters B*, 246(3):377 – 384, 1990. 21

[58] Graldine Servant and Tim M.P. Tait. Is the lightest kaluzaklein particle a viable dark matter candidate? *Nuclear Physics B*, 650(1):391 – 419, 2003. 21

[59] Hsin-Chia Cheng, Jonathan L. Feng, and Konstantin T. Matchev. Kaluza-klein dark matter. *Phys. Rev. Lett.*, 89:211301, Oct 2002. 21

[60] Dan Hooper and Stefano Profumo. Dark matter and collider phenomenology of universal extra dimensions. *Physics Reports*, 453(2):29 – 115, 2007. 21

[61] Gianfranco Bertone, Géraldine Servant, and Günter Sigl. Indirect detection of kaluza-klein dark matter. *Phys. Rev. D*, 68:044008, Aug 2003. 21

[62] John McDonald. Gauge singlet scalars as cold dark matter. *Phys. Rev. D*, 50:3637–3649, Sep 1994. 21

[63] C.P. Burgess, Maxim Pospelov, and Tonnis [ter Veldhuis]. The minimal model of nonbaryonic dark matter: a singlet scalar. *Nuclear Physics B*, 619(1):709 – 728, 2001. 21

[64] Robert Schabinger and James D. Wells. Minimal spontaneously broken hidden sector and its impact on higgs boson physics at the cern large hadron collider. *Phys. Rev. D*, 72:093007, Nov 2005. 21

[65] Matthew T Bowen, Yanou Cui, and James D Wells. Narrow trans-TeV higgs bosons andH→hhdecays: two LHC search paths for a hidden sector higgs boson. *Journal of High Energy Physics*, 2007(03):036–036, mar 2007. 21

[66] Christoph Englert, Tilman Plehn, Dirk Zerwas, and Peter M. Zerwas. Exploring the higgs portal. *Physics Letters B*, 703(3):298 – 305, 2011. 21

[67] John March-Russell, Stephen M West, Daniel Cumberbatch, and Dan Hooper. Heavy dark matter through the higgs portal. *Journal of High Energy Physics*, 2008(07):058–058, jul 2008. 21

[68] Eduardo Pontón and Lisa Randall. TeV scale singlet dark matter. *Journal of High Energy Physics*, 2009(04):080–080, apr 2009. 21

[69] Daniel J. H. Chung, Edward W. Kolb, and Antonio Riotto. Superheavy dark matter. *Phys. Rev. D*, 59:023501, Nov 1998. 21

[70] Daniel J. H. Chung, Edward W. Kolb, and Antonio Riotto. Production of massive particles during reheating. *Phys. Rev. D*, 60:063504, Aug 1999. 21

[71] Daniel J. H. Chung, Edward W. Kolb, and Antonio Riotto. Nonthermal supermassive dark matter. *Phys. Rev. Lett.*, 81:4048–4051, Nov 1998. 21

[72] Daniel J. H. Chung, Patrick Crotty, Edward W. Kolb, and Antonio Riotto. Gravitational production of superheavy dark matter. *Phys. Rev. D*, 64:043503, Jul 2001. 21

[73] Francesco Caracciolo, Alberto Parolini, and Marco Serone. UV completions of composite Higgs models with partial compositeness. *Journal of High Energy Physics*, 2013(2):66, feb 2013. 22

[74] Michele Redi and Andreas Weiler. Flavor and CP invariant composite Higgs models. *Journal of High Energy Physics*, 2011(11):108, nov 2011. 22

[75] Stefania De Curtis, Michele Redi, and Andrea Tesi. The 4D composite Higgs. *Journal of High Energy Physics*, 2012(4):42, apr 2012. 22

[76] Michele Frigerio, Alex Pomarol, Francesco Riva, and Alfredo Urbano. Composite scalar dark matter. *Journal of High Energy Physics*, 2012(7):15, jul 2012. 22

[77] Mikael Chala. h$\gamma\gamma$ excess and dark matter from composite Higgs models. *Journal of High Energy Physics*, 2013(1):122, jan 2013. 22

[78] Jihn E. Kim, Bumseok Kyae, and Hyun Min Lee. Wave function of the radion in the brane background with a massless scalar field and a self-tuning problem. *Phys. Rev. D*, 66:106004, Nov 2002. 24

[79] Csaba Csáki, Jay Hubisz, and Seung J. Lee. Radion phenomenology in realistic warped space models. *Phys. Rev. D*, 76:125015, Dec 2007. 24

[80] Chengcheng Han, Hyun Min Lee, Myeonghun Park, and Verónica Sanz. The diphoton resonance as a gravity mediator of dark matter. *Physics Letters B*, 755:371–379, apr 2016. 25, 39, 40

[81] Barry M. Dillon, Chengcheng Han, Hyun Min Lee, and Myeonghun Park. KK graviton resonance and cascade decays in warped gravity. *International Journal of Modern Physics A*, 32(33):1745006, nov 2017. 25

[82] Thomas D Rueter, Thomas G Rizzo, and JoAnne L Hewett. Gravity-mediated dark matter annihilation in the Randall-Sundrum model. *Journal of High Energy Physics*, 2017(10):94, oct 2017. 25

[83] Marco Cirelli, Eugenio Del Nobile, and Paolo Panci. Tools for model-independent bounds in direct dark matter searches. *Journal of Cosmology and Astroparticle Physics*, 2013(10), 2013. 27, 35

[84] L. B. Kobzarev, I. and Okun. GRAVITATIONAL INTERACTION OF FERMIONS. *Zh. Eksp. Teor. Fiz.*, 43:1904–1909, 1962. 27

[85] Avinash Khare and John Oliensis. Constraints on the Interactions of Majorana Particles From {CPT} Invariance. *Physical Review D*, 29(7):1542–1543, apr 1984. 27

[86] Zainul Abidin and Carl E. Carlson. Nucleon electromagnetic and gravitational form factors from holography. *Physical Review D - Particles, Fields, Gravitation and Cosmology*, 79(11), 2009. ix, 27, 29, 30

[87] Manuel Drees and Mihoko M. Nojiri. Neutralino-nucleon scattering reexamined. *Physical Review D*, 48(8):3483–3501, oct 1993. 28

[88] Junji Hisano, Koji Ishiwata, Natsumi Nagata, and Masato Yamanaka. Direct Detection of Vector Dark Matter. *Progress of Theoretical Physics*, 126(3):435–456, sep 2011. viii, 28, 29

[89] Richard J Hill and Mikhail P Solon. Standard Model anatomy of WIMP dark matter direct detection. II. QCD analysis and hadronic matrix elements. *Physical Review D - Particles, Fields, Gravitation and Cosmology*, 91(4), 2015. 28

[90] Johannes Hirn and Verónica Sanz. A Negative S parameter from holographic technicolor. *Physical Review Letters*, 97(12):121803, sep 2006. 29

[91] Nikhil Anand, A Liam Fitzpatrick, and W C Haxton. Weakly interacting massive particle-nucleus elastic scattering response. *Physical Review C*, 89(6):065501, jun 2014. 35, 36

[92] E. Aprile et al. First Dark Matter Search Results from the XENON1T Experiment. *Physical Review Letters*, 119(18):181301, oct 2017. 38, 41

[93] D. S. Akerib et al. Results from a Search for Dark Matter in the Complete LUX Exposure. *Physical Review Letters*, 118(2):021303, jan 2017. 38

[94] J. Angle et al. Search for Light Dark Matter in XENON10 Data. *Physical Review Letters*, 107(5):051301, jul 2011. 38

[95] The ATLAS Collaboration. Search for new light resonances decaying to jet pairs and produced in association with a photon or a jet in proton-proton collisions at $s = 13$ TeV with the ATLAS detector. Technical report, 2016. 41

[96] Felix Kahlhoefer, Suchita Kulkarni, and Sebastian Wild. Exploring light mediators with low-threshold direct detection experiments. *Journal of Cosmology and Astroparticle Physics*, 2017(11):016–016, nov 2017. 42